Available online at www.sciencedirect.com
ScienceDirect
Journal of Sound and Vibration 318 (2008) 625–654
JOURNAL OF SOUND AND VIBRATION
www.elsevier.com/locate/jsvi

Review

Aeroacoustics research in Europe: The CEAS-ASC report on 2007 highlights

H.H. Brouwer[a,*], S.W. Rienstra[b]

[a]National Aerospace Laboratory NLR, Voorsterweg 31, 8316 PR Marknesse, The Netherlands
[b]Eindhoven University of Technology, Den Dolech 2, 5600 MB Eindhoven, The Netherlands

Received 8 July 2008; accepted 15 July 2008
Handling Editor: C.L. Morfey
Available online 6 September 2008

Abstract

The Council of European Aerospace Societies (CEAS) Aeroacoustics Specialists Committee (ASC) supports and promotes the interests of the scientific and industrial aeroacoustics community on a European scale and European aeronautics activities internationally. In this context, "aeroacoustics" encompasses all aerospace acoustics and related areas. Each year the committee highlights some of the research and development projects in Europe.

This paper is a report on highlights of aeroacoustics research in Europe in 2007, compiled from information provided to the ASC of the CEAS.

During 2007, numerous research programmes were funded by the European Union. Some of the contributions submitted to the editor summarize selected findings from these programmes, while other articles cover issues supported by national associations. Furthermore, a concise summary of the workshop on "Experimental and Numerical Analysis and Prediction of Combustion Noise" held in Lisbon in September, is included in this report. Enquiries concerning all contributions should be addressed to the authors who are given at the end of each subsection.

Contents

*Corresponding author. Tel.: +31 527 248653; fax: +31 527 248210.
E-mail address: brouwer@nlr.nl (H.H. Brouwer).

0022-460X/$ - see front matter © 2008 Elsevier Ltd. All rights reserved.
doi:10.1016/j.jsv.2008.07.020

1. CEAS-ASC workshop

The workshop on "Experimental and Numerical Analysis and Prediction of Combustion Noise" was held on 27–28 September 2007 at the Congress Center of Instituto Superior Técnico. It was the 11th Workshop sponsored by the Aeroacoustics Committee of CEAS and the first to be sponsored as well by the Aeroacoustics Committee of AIAA. The organizers were Wolfgang Schröder from RWTH Aachen and Luis Campos from IST, who will act as Guest Editors of a special issue of International Journal of Aeroacoustics dedicated to the workshop.

The subject of "Combustion Noise" has gained increasing importance recently, as progress in other areas of sound reduction makes this type of sound source more relevant. The interest in the subject was demonstrated by the 90 attendants and presentation of 29 papers over two days. Each day started with an invited review, viz. "Flame Dynamics and Combustion Noise" by Sebastien Candel and co-workers from Ecole Centrale de Paris on the first day, and on the second "Large Eddy Simulation of Combustion Noise" by Heinz Pitsch and co-workers from Stanford University.

There is a strong resurgence of interest in "entropy noise", following a long hiatus since the pioneering work of Marble, Candel, Howe and others in the seventies and eighties. The traditional subjects of combustion instability and acoustic-combustion coupling have if anything gained in importance due to the application in

jet and rocket engines and industrial burners. The progress in Computational Fluid Dynamics (CFD) and Computational Aeroacoustics (CAA) in evident as in other areas. The stage has been reached where it is already possible to combine detailed chemistry analysis with flow and acoustic computations. This may be a major trend for the future.

Written by Luis Campos: luis.campos@ist.utl.pt, IST, Portugal.

2. European-funded projects

2.1. SILENCE(R)

SIgnificantly Lower community Exposure to aircraft NoiSE (SILENCE(R)) has been the largest European Commission research project dedicated to aircraft noise reduction. It was budgeted at 112 million euros, and brought together 51 partners. Research spanned several main areas, including engine and airframe source noise, nacelle technologies and active control.

Combined with innovative low-noise operational procedures studied in parallel, the project has achieved an impressive 5 dB noise reduction. This meets the medium-term objective of the European Commission's PCRD R&D Framework Programs, and marks a significant advance towards ACARE's research goal of a 10 dB reduction in aircraft noise by 2020.

SILENCE(R) has met its goal of validating large-scale noise reduction solutions concerning the engine (aeroacoustic design, active technologies), nacelle (aeroacoustic design, innovative acoustic treatment, active noise control), and airframe (aeroacoustic design). More than 35 prototypes were tested as part of the SILENCE(R) program, along with studies of improved operational procedures to reduce aircraft noise.

2.1.1. Engine source noise

The research on engine noise spanned the fan, compressor, turbine and jet noise. A low-noise compressor was designed using CFD by modifying the inlet guide vanes and the first stator of an existing large-scale compressor model. With the new design, the sound power level of the first rotor blade passing frequency tone was significantly reduced under the appropriate operating conditions. This reduction was achieved without compromising the aerodynamic and mechanical characteristics of the compressor.

Low-noise fan designs were developed for both high bypass ratio (HBR) and ultra-high bypass ratio (UHBR) engine concepts, by capitalizing on computational aeroacoustic multidisciplinary design optimization techniques. Advanced designs for the HBR engines have undergone large-scale tests at the AneCom Aerotest Facility.

Researchers also tested the acoustic and aerodynamic performance of alternative exhaust nozzle shapes designed to reduce jet noise, using Onera and QinetiQ facilities, as well as an Airbus A320 flying test bed. After down selecting from the numerous designs tested on model scale, the Squid nozzle design was build on full scale and tested in-flight as well as on an acoustic ground based outdoor test bed (see Fig. 1).

2.1.2. Nacelle technologies

Research focussed on both the nacelle geometry and acoustic liners

One design possibility for a low-noise nacelle was a negatively scarfed inlet (NSI), a concept that is intended to change the directional pattern of the radiated engine noise, so that more noise will be directed upward, and less noise downward. After extensive wind-tunnel testing on scale models at Onera, flight tests were made with an NSI mounted on one of the engines of an Airbus A320 at Moron (Spain) and Tarbes (France) (see Fig. 2).

The noise benefit of extending the acoustic liner over the intake lip was demonstrated on a static test of a Rolls-Royce Trent prototype and in flight on the A320 on a CFM56 engine inlet.

Research on nacelle acoustic liners included the development and assessment of zero-splice inlet liners. Large-scale research on zero-splice inlet liners has been conducted on the Trent engine.

To reduce turbine and combustor noise, the project expended considerable effort on the investigation of innovative absorbent materials and concepts capable of resisting the high temperatures of the engine core exhaust flow. Several full-scale prototypes were manufactured and tested, using "hot stream" solutions in the primary nozzle and the engine centerbody.

Fig. 1. Squid nozzle on A320/CFM56.

Fig. 2. Negatively scarfed inlet.

2.1.3. Airframe source noise

The extensive airframe noise tests for SILENCE(R) focused on technologies to reduce landing gear noise and noise generated by high-lift devices. Flight tests were carried out on an Airbus A340 with landing gear fitted with low-noise fairings.

For future applications, more comprehensive changes to the landing gear configuration may be needed to reduce noise. Full-scale experiments have been carried out on these concepts in a wind tunnel at DNW.

2.1.4. Active control

Several active and adaptive technologies are under investigation. These technologies are based on either anti-noise cancellation techniques or self-adapting technologies to provide maximum noise reduction depending on flight conditions. Examples include active stator technology and active control of buzz-saw tones, for which large-scale tests were carried out successfully at the RACE and ANECOM anechoic fan noise facilities. The most promising results were generated by the active stator technology (see Fig. 3).

Written by Eugène Kors: eugene.kors@snecma.fr, Snecma, France.

Fig. 3. Active stator.

2.2. SEFA

Sound engineering for aircraft (SEFA) was the first project to use Sound Engineering to define optimum aircraft community noise "shapes" (characteristics to design target sounds). Sound design metrics were derived by the subjective assessment of overflying aircraft noise events within extensive psychometric listening tests in 8 different laboratories. The Paired Comparison Test and Semantic Differential Test methods have been shown to be acceptable to describe the human perception of current aircraft sounds. From these extensive tests, the following lessons have been learned:

- Differentiation and scaling of aircraft sounds are very difficult for a typical listener. One of the reasons is that full overflying events are continuously changing over a period of typically 40 s.
- The importance, as a disturbing feature, of any particular sound characteristics (e.g., fan tones) is largely dependent on the entire sound composition of an overflying event, i.e., on a number of other tonal and broadband components.
- Characterising target sound generally has been shown to have more dimensions than anticipated at the beginning of SEFA.

Due to the fact that the derived target sounds were specific to the aircraft type, it was not possible to define general aircraft design guidelines within SEFA. However, guidelines taking into account airframe design, engine design and flight procedures have been derived according to aircraft-specific features. Therefore, SEFA has provided valuable information on how the noise annoyance of aircraft can be reduced, not only by lowering noise levels, but also by improving the characteristics of aircraft noise signatures.

Written by Roger Drobietz: Roger.Drobietz@eads.net, EADS-IW, Germany.

2.3. PROBAND

Fan broadband noise is a major aircraft noise challenge now, and will be even more important in the future. Novel low-noise engine architectures, such as ultra-high-bypass-ratio engines and lower-speed fans, can help address jet noise and fan tone noise, but previous EC-funded programmes have shown they are unlikely to reduce significantly fan broadband noise without improved understanding of the source mechanisms. The advances in numerical methods, which have revolutionised tone noise prediction, have yet to make an equivalent impact on broadband noise prediction. Improvement of Fan Broadband Noise Prediction (PROBAND) addresses these issues by providing industry with an improved understanding of the broadband

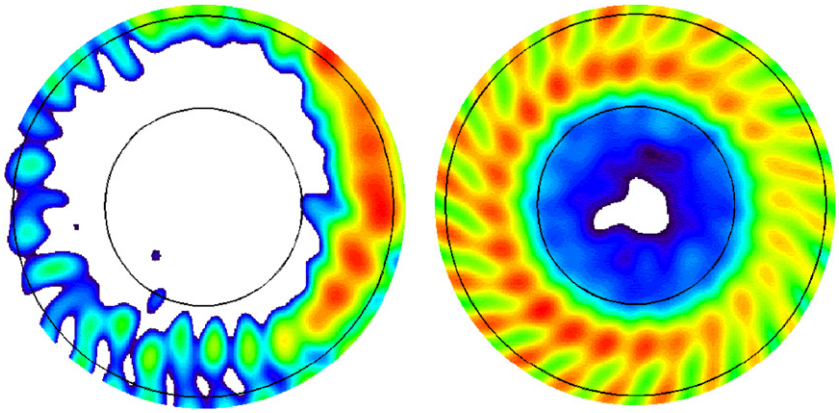

Fig. 4. Broadband noise source maps on fan stage stator (left) and rotor (right).

noise source mechanisms, with validated broadband noise prediction methods, and with low fan broadband noise concepts.

PROBAND exploits the noise technology and methodology acquired in EC-funded projects and national programmes, to develop methods for the design of a fan system of sufficiently low broadband noise to meet the EU noise level targets.

The project is subdivided into three technical workpackages (WPs). In WP2, single source studies and model development take place. Selected major results of WP2 can be found in Refs. [1–4]. WP3 consists of laboratory scale fan rig tests using novel measurement techniques supported by cutting edge CFD prediction approaches. First experimental results are published in Ref. [5]. In WP4, the developed methods will be validated and their application will be demonstrated on an industrial Fan-OGV rig test. One experimental method was already published [6]. Fig. 4 depicts an analysis result applying this novel in-duct beamforming technique on a fan inlet sound field.

Written by Lars Enghardt,lars.enghardt@dlr.de, DLR, Germany.

3. Airframe noise

3.1. Trailing-edge noise research

From Ffowcs-Williams and Hall [7] it is known that the noise generation mechanism of trailing-edge (TE) scattering noise, i.e. an edge-enhanced conversion of turbulence into sound, is directly related to the geometric discontinuity at the TE. It is concluded that a "smoothed" TE boundary condition, by flow-permeable edge-modifications, will reduce TE noise radiation efficiency. In search of applicable retrofit solutions for existing airframe components the principal noise reduction capability of comb-type edge-modifications was proven at different two-dimensional test airfoils ($Re = 1.1–7.9$ Mio). Fig. 5 shows the noise reduction potential (2–10 dB) of several TE modifications. Basic design rules and scaling laws for a low-noise TE design were derived [8]. A major finding was that comb design optimization is mainly determined by design details of the comb-device (i.e. material flexibility and dimensions), rather than the incident flow. Extensive reference measurements at different solid TE geometries provided a database for validating various available TE noise prediction approaches. Fig. 6 compares measured data (0.4-m chord NACA0012-like airfoil with a 0.15-mm TE thickness) with the results of (1) a semi-empirical TE noise prediction according to Brooks, Pope and Marcolini (BPM) [9,10], with neglected TE bluntness, and (2) a CAA simulation, based on a stochastic approach (RPM) [11], as implemented in DLR's PIANO code, for a 0.2-m chord infinitely thin flat plate ($Re = 550{,}000$, absolute levels calibrated with the measurement data).

Written by Michaela Herr, michaela.herr@dlr.de, DLR, Germany.

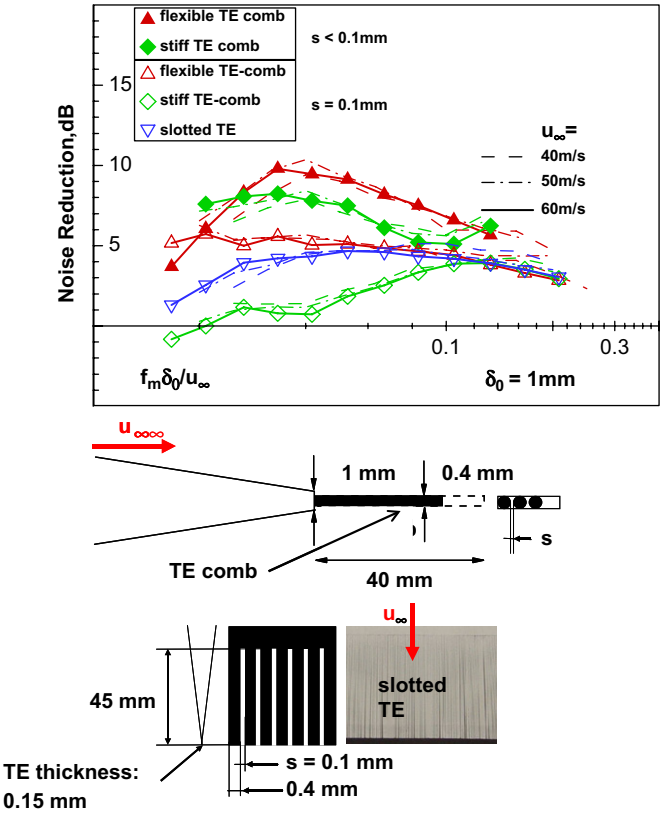

Fig. 5. Noise reduction by comb-type TE-modifications (reference data in Fig. 6).

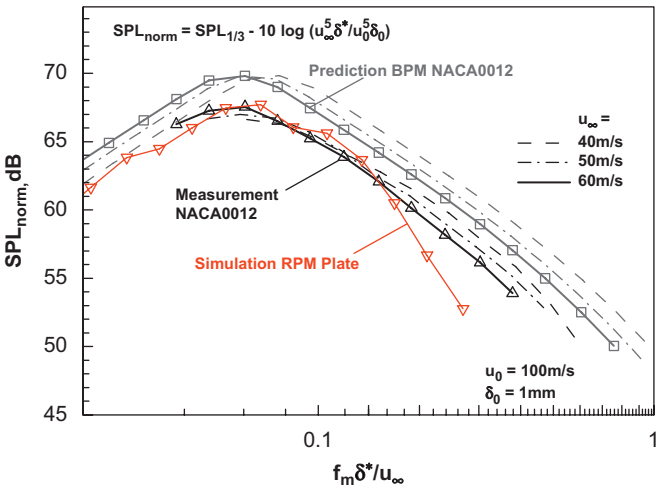

Fig. 6. Comparison of (solid reference) TE noise measurements and predictions.

3.2. *Numerical synthesis of airframe noise for aircraft sound engineering*

As part of the SEFA project (see Section 2.2), the airframe noise of civil transport aircraft has been numerically evaluated and compared with measurements taken in some European airports, in order to

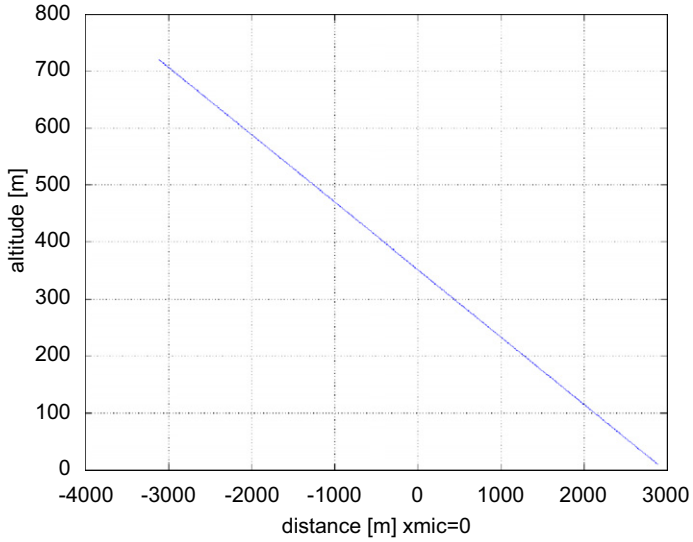

Fig. 7. Landing path of a civil airplane.

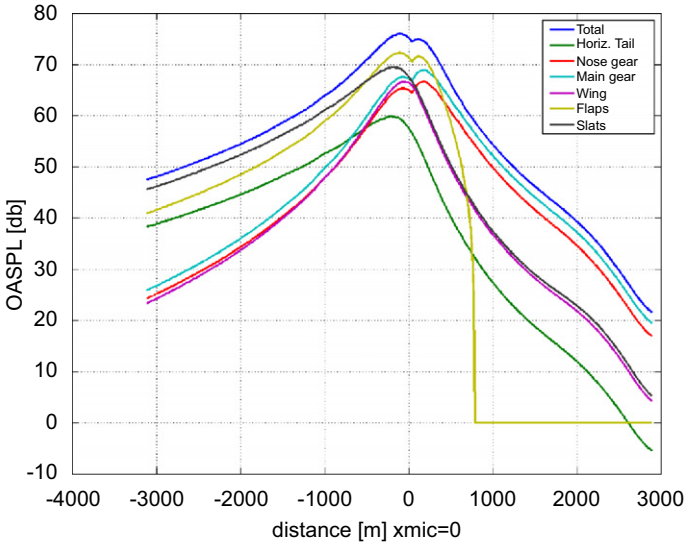

Fig. 8. OASPL at receiver location and its breakdown into components.

separate the airframe noise from other noise components of a typical aircraft [12]. Priority was given to airframe noise because it sets a lower limit below which reduction of engine noise has no significant effect on the overall flyover noise level. Figs. 7 and 8 show the landing path of a typical civil aircraft and its numerically produced sound pressure levels. The generated sounds have been used for psychometric tests, where the real conditions are reproduced in laboratory without the need for expensive measurement campaigns. These sounds are easily modified for changing aircraft geometry and operation conditions.

Written by G. Scarselli, scarsell@unina.it, University of Naples "Federico II", Italy.

4. Fan and jet noise

4.1. Simulation of sound emission by turbulent flows

Promising results from Detached Eddy Simulation (DES) were obtained for the simulation of sound emission by turbulent flows. DES is a hybrid RANS-LES method positioned between conventional RANS and LES methods in terms of computational costs and predictive accuracy, particularly suitable to include geometric modifications. DES was applied to the prediction of jet-mixing noise from serrated "chevron" nozzles. A short-cowl (staggered) and a long-cowl (internal mixing) nozzle have been studied in the European CoJeN research project [13] and the German national program FREQUENZ [14], respectively. The effect of serrations on the flow field behind the long-cowl nozzle is shown using isosurfaces of the λ_2 vortex core criterion in Fig. 9 (left), from which the serrations are seen to force an earlier development of three-dimensional turbulence. Fig. 9 (right) shows the far-field directivities of the serrated nozzle in comparison with the baseline nozzle. The predictions for the baseline case agree with the experimental data to within 2 dB and the serrations yield a noise reduction in all directions.

Written by Ulf Michel, Łukasz Panek, Dandy Eschricht, Jianping Yan, Charles Mockett, Frank Thiele, frank.thiele@cfd.tu-berlin.de, TU Berlin, Germany.

4.2. LES simulation of chevron nozzle acoustics

Implicit Large Eddy Simulations (LES) of the flow and acoustic field around chevroned nozzles have been compared with NASA Glenn measurements [15] for nozzles with around 6° (SMC1) and 18° (SMC6) chevron penetration. Turbulent statistics of sufficient quality gave reasonable far field sound predictions using the Ffowcs Williams-Hawking approach. Fig. 10 gives flow field isosurfaces for the SMC1 geometry. Fig. 11 gives the far field sound level for the SMC0 (no chevron) and SMC1 and SMC6 geometries with the unstructured FLUXp CFD code.

Written by P. Tucker, H. Xia, S. Eastwood, Whittle Laboratory, pgt23@cam.ac.uk, hx222@cam.ac.uk, se282@cam.ac.uk, The University of Cambridge, UK.

4.3. 3D simulations of installation effects on turbofan engine AftFan noise

Several experimental and numerical studies were recently conducted at ONERA, aiming at characterizing the shielding effect provided by an empennage wing, on the aft fan noise of a coaxial engine. The numerical studies were done by the sAbrinA solver (Refs. [16,17]), performing both aerodynamics (CFD) and

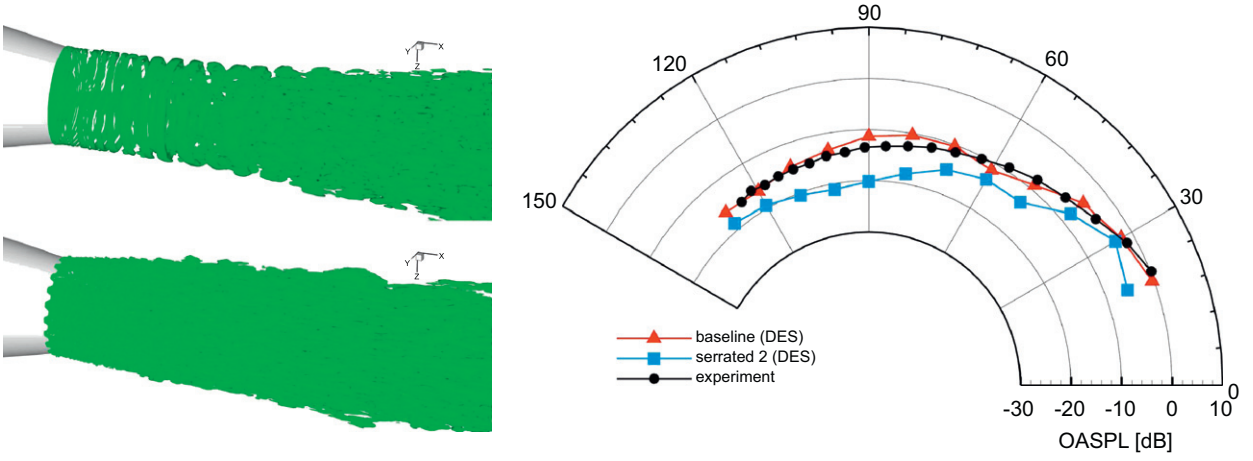

Fig. 9. Left: comparison between flow field structures of the baseline (above) and serrated (below) nozzle. Right: predicted overall sound pressure levels in the far field for the long-cowl nozzle with and without serrations in comparison to measurements for the baseline case.

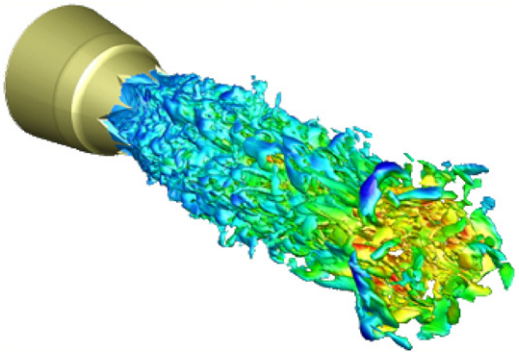

Fig. 10. Flow field isosurfaces for SMC1 geometry.

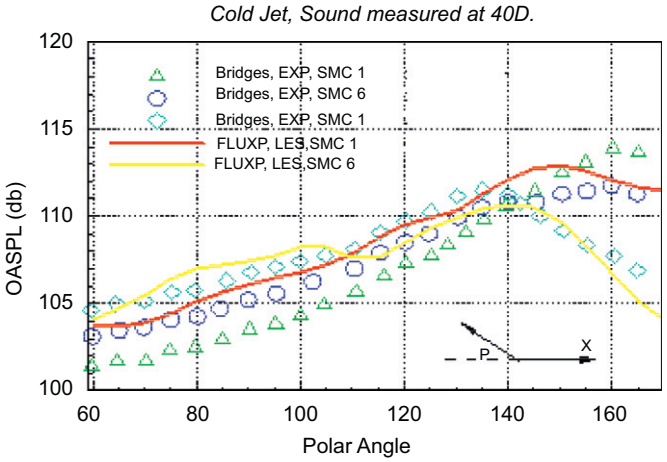

Fig. 11. Far field OASPL for chevron nozzle.

aeroacoustics (CAA) calculations. 3D aft fan noise propagation and radiation was simulated for a coaxial engine, installed over an empennage airfoil and being affected by realistic "take-off" thermodynamic conditions (viz. a highly heterogeneous jet mean flow). Fig. 12 presents the near-field CAA results [18] obtained for an acoustic mode (with azimuthal and radial orders of 2) at 0.5 BPF in the upstream region of the secondary exhaust. It turns out that the airfoil acts as an efficient shield, as only a fraction of the sound emitted in the downward direction is diffracted by the airfoil and propagates towards the ground.

Written by S. Redonnet, G. Desquesnes & E. Manoha, stephane.redonnet@onera.fr, ONERA, France.

4.4. Noise reduction by impinging microjets

The effects of fluidic control on the aeroacoustic characteristics of a Mach 0.9 high-Reynolds axisymmetric jet are investigated experimentally [19]. The air-microjet system comprised up to 36 impacting microjets directed towards the jet centerline (Fig. 13), and was designed to modify various microjet parameters. A significant noise reduction was obtained for the entire range of noise emission angle θ (Fig. 14). The dependency was studied of the reduction with respect to the outgoing mass flux per microjet, the number of microjets and their layout in the azimuth of the main jet. The global noise reduction varied from 0 to 1.8 dB, showing some non-monotonic behavior caused by the change from subsonic to supersonic regimes of the microjets. In small numbers, the microjets act independently. This was confirmed by aerodynamic studies by Stereoscopic Particle Image Velocimetry. These studies [19,20] indicate a strong correlation between the maximum level of turbulence just behind the nozzle exit and the high-frequency noise, which was previously

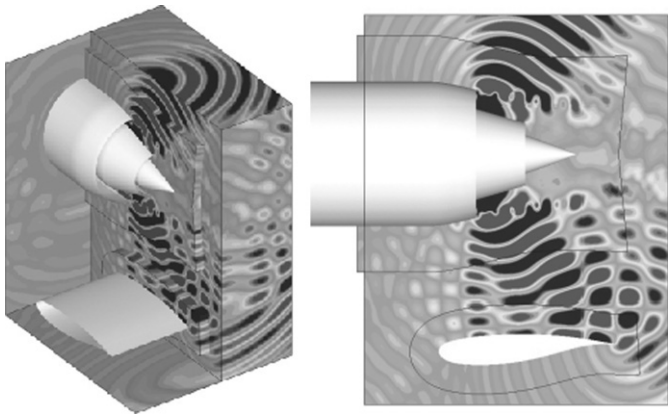

Fig. 12. 3D numerical simulation of the acoustic installation effects to noise from a coaxial exhaust, installed over an empennage airfoil, with respect to a particular aft fan noise content (mode (2, 2) at 1/2 BPF) and a given jet mean flow (take-off flight). The acoustic shielding due to the airfoil is highlighted by the acoustic attenuation (resp. reinforcement) on the lower (resp. upper) side of the profile.

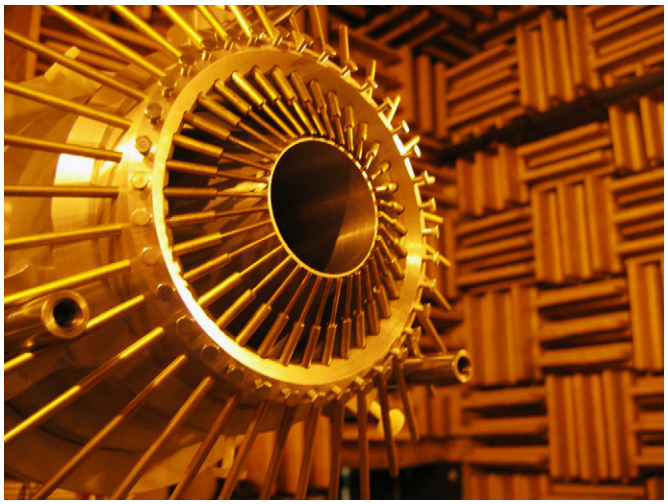

Fig. 13. Air-microjet system in the anechoic wind tunnel of Ecole Centrale de Lyon.

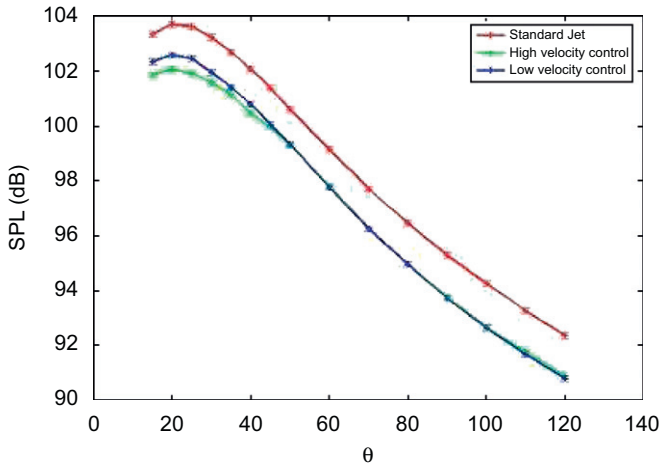

Fig. 14. Acoustic directivity measured for three configurations.

shown to potentially outweigh the acoustic benefits obtained for lower frequencies. The maximum level of turbulence measured at the longitudinal position corresponding to half the potential core length was shown to be also highly correlated to the jet noise reduction.

Written by Th. Castelain and Daniel Juvé, thomas.castelain@ec-lyon.fr, Ecole Centrale, Lyon, France.

4.5. Jet noise simulation using a hybrid method

Jet noise of several nozzle configurations and operating points have been computed by means of a hybrid method, combining a CFD/LES aerodynamic computation and an acoustic integral formulation (Ffowcs-Williams and Hawkings) for the far field radiation. Influence of temperature and micro-jets have been investigated on a single stream nozzle and computations on realistic industrial configurations have also been performed. A hybrid mesh approach had been chosen, combining the simplicity of unstructured elements for complex geometries and the precision of hexahedrons for the jet development. This approach produced realistic jet flows although the potential cores were too short and the far field sound pressure levels were overestimated compared to measurements. These discrepancies could be due to the under-resolution of the mesh. Parameter effects such as temperature and micro-jets, show a qualitatively correct behavior (see Fig. 15).

Theoretical work on the quadrupole volume integral demonstrated the feasibility of noise prediction using volume integral methods, see Figs. 16 and 17 [21,22].

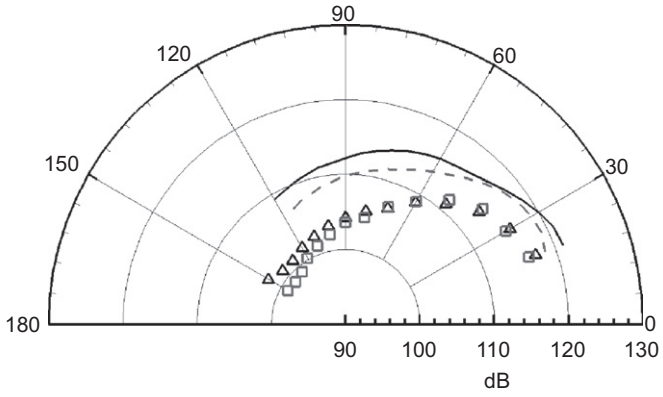

Fig. 15. OASPL at 30 diameters from the nozzle. – cold jet computation, -- hot jet computation, Δ cold jet measurement, □ hot jet measurement.

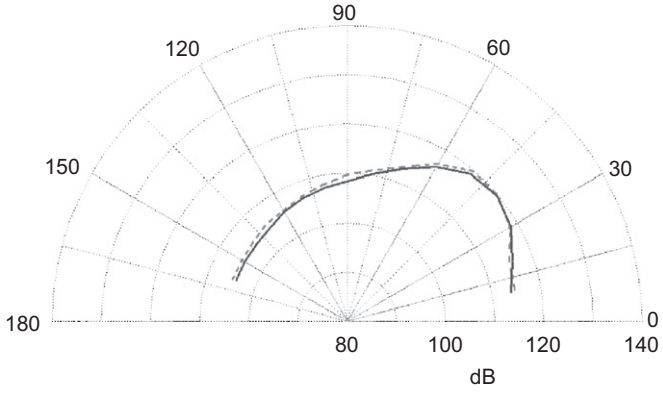

Fig. 16. Comparison of the OASPL for: – the surface method (F-WH) and -- the volume method (Lighthill).

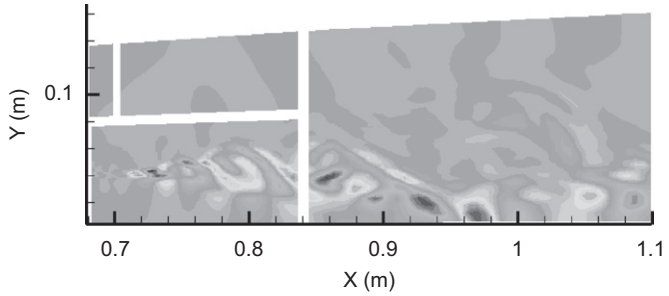

Fig. 17. Visualization of the instantaneous volume noise sources inside de jet.

Written by M. Huet, F. Vuillot, N. Lupoglazoff, G. Perez, J. Prieur, G. Rahier, Maxime.Huet@onera.fr, ONERA, France.

5. Techniques and methods in aeroacoustics

5.1. Aero-acoustic modeling of subsonic confined flows using an active bi-port formulation

The transmission characteristics (4-pole parameters) of two expansion chambers placed behind each other are determined using a time-domain two-load technique with a plane pulse excitation, using a Linearized Euler model [23] (Fig. 18). Based on the four pole parameters the noise generating mechanisms (active part) are determined using compressible Large Eddy Simulations (LES) [24,25] (Fig. 19). Since hydrodynamic pressure oscillations (pseudo-sound) are present behind the expansion chambers, an aerodynamic/acoustic splitting technique [26,27] is used to separate the aerodynamic and the acoustic fluctuating field.

Written by W. De Roeck, V. Solntseva & W. Desmet, wim.deroeck@mech.kuleuven.be, Katholieke Universiteit Leuven, Belgium.

5.2. Application of hybrid methods to high frequency aeroacoustics

In hybrid methods for calculation of aerodynamic sound generation, computation of the flow is decoupled from computation of the sound propagation. These methods are especially suitable for high Reynolds, low Mach number flows. Although hybrid methods have proved their efficiency only for low frequencies (Helmholtz numbers), an innovative procedure is proposed [28] to compute the noise for the whole frequency spectrum from the same CFD computation. The procedure is tested for an infinite span airfoil placed in a turbulent round jet (Fig. 20). The chord based Reynolds number is 36,000 and the Mach number is 0.04. The unsteady, three-dimensional incompressible flow around the airfoil is first computed with the LES module of CFD solver Fluent. In a second step, the unsteady pressure data along the airfoil surface were used through the Sysnoise solver implementing Curle's analogy to obtain the radiated sound. The found predictions exhibit a very similar slope of the spectrum (compared to experiments), with, however, an overall under-prediction of about 4–6 dB in the meaningful frequency range (100–800 Hz), see Fig. 21.

Written by J. Christophe and J. Anthoine, anthoine@vki.ac.be, VKI, Belgium.

5.3. CAA prediction of broadband trailing-edge and jet noise

Significant progress has been made in the modeling of trailing-edge as well as jet noise sources as part of a fast aeroacoustic prediction model for broadband noise (DLR's CAA code PIANO). The simulation of trailing-edge noise is based on vortex sound sources, computed from synthetic turbulence based on the Random-Particle Mesh method (RPM), [11]. Fig. 6 (Section 3.1) shows a one-third octave spectrum compared with measurements [8]. The spectrum is predicted very accurately up to Strouhal numbers of 0.17, corresponding to the spectral resolution of the CAA mesh. For the prediction of jet noise, the noise source of

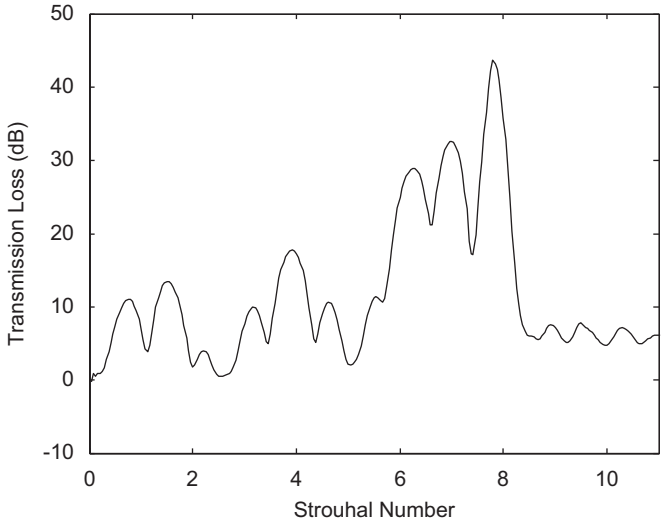

Fig. 18. Transmission loss (dB) for 2 expansion chambers placed behind of each other.

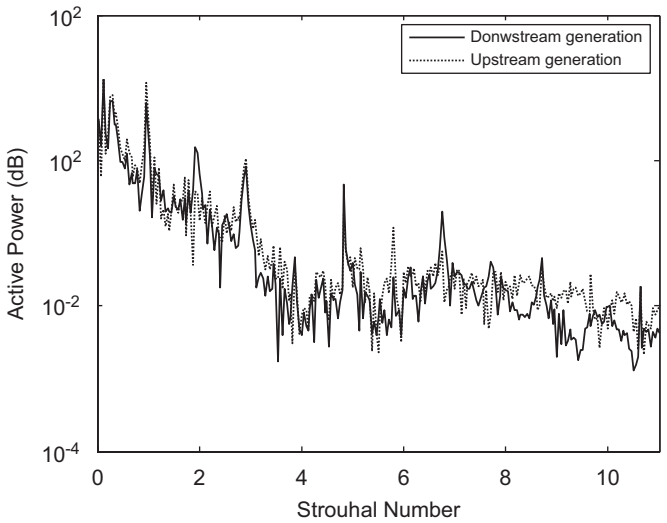

Fig. 19. Active noise generation is downstream and upstream direction for 2 expansion chambers placed behind of each other.

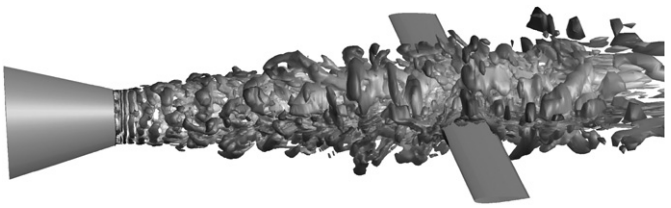

Fig. 20. Instantaneous flow field around the airfoil, coherent structures visualized with the second invariant of the velocity gradient tensor $Q = 30{,}000$ colored by dynamic pressure.

Tam & Auriault [29] is realized with the RPM method in the time-domain [30]. This source models broadband fine-scale turbulence noise in the frequency domain. In the RPM time domain realization of the respective forcing of the linear or non-linear Euler equations not only the fine scale turbulence related sound is predicted

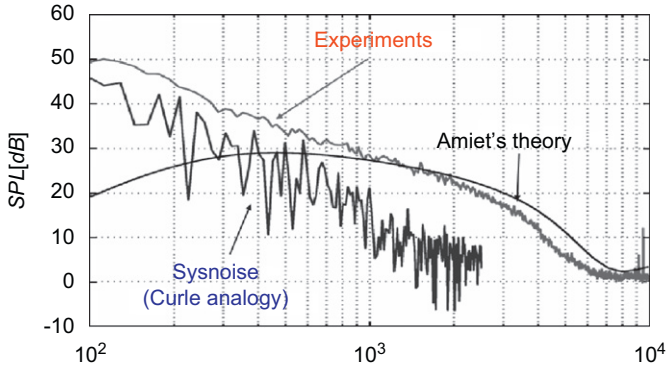

Fig. 21. Comparison of experimental and predicted sound pressure levels.

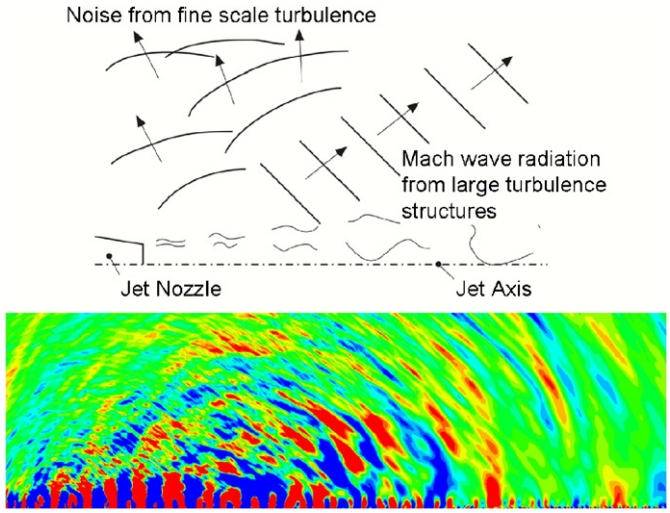

Fig. 22. CAA Simulation of jet noise based on stochastic sound sources.

but also large scale turbulence noise due to the excitation of instability waves in the jet. Fig. 22 shows a snapshot of the pressure field from jet computations. Large scale sound waves are predominantly radiated under an angle of approx. 160° from the upstream jet axis, whereas fine-scale turbulence noise is radiated more omni-directional. Fig. 23 presents a comparison of CAA spectra at 90° and 160° receiver position with the universal f- and g-noise spectra derived by Tam et al. [31] from large experimental data sets. The CAA spectra show a very close agreement with the corresponding universal spectra.

Written by Roland Ewert, roland.ewert@dlr.de, DLR, Germany.

5.4. Direct aeroacoustic simulations of a supersonic jet with the STE-DG method

The Space-Time-Expansion Discontinuous Galerkin (STE-DG) method by Gassner et al. [32,33], has been applied to the simulation of supersonic jet noise. Both the flow field and the propagation of the acoustic waves into the far field are contained in one single computation, which is non-trivial due to the multi-scale problem of aeroacoustics. Because of the small dimensions of the nozzle, a DNS simulation of the jet ($Ma = 1.4$, $Re = 150{,}000$) is possible with grid cell sizes near the Kolmogorov length. The implementation of the method is of arbitrary order in space and time. As DG cells are able to represent polynomial information inside one single element, relatively coarse grids can be used. Due to its locality, the DG method is able to achieve

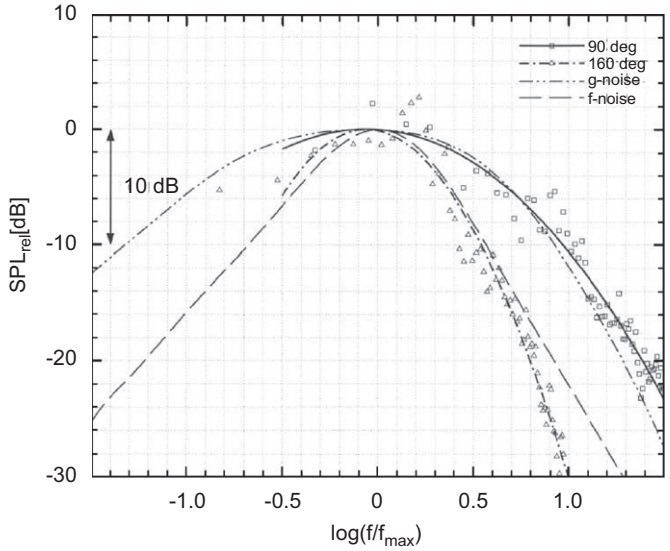

Fig. 23. Comparison of CAA spectra with universal large-scale (f-noise) and small-scale (g-noise) spectra.

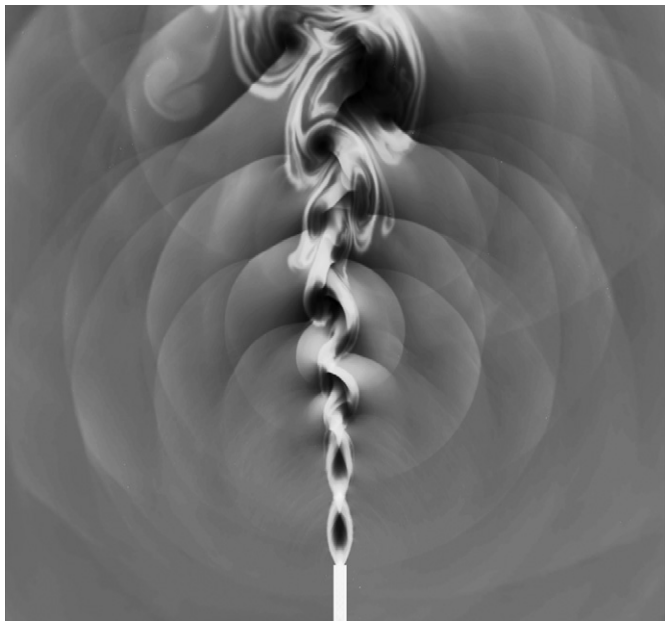

Fig. 24. 2D simulation of a jet, including the mach discs, vortices and the acoustic waves.

high-order of accuracy on unstructured grids. Fig. 24 shows the zoom into a 2D simulation of the jet, including the mach discs, vortices and the acoustic waves.

Written by C.-D. Munz, C. Altmann, G. Gassner, F. Lörcher, munz@iag.uni-stuttgart.de, Universität Stuttgart, Germany.

5.5. A 3D numerical method for studying poroelastic liners with mean flow

The finite element (FE) method is used to study noise attenuation by poroelastic materials exposed to grazing flow. The acoustic propagation in the liner and in the fluid domain are respectively

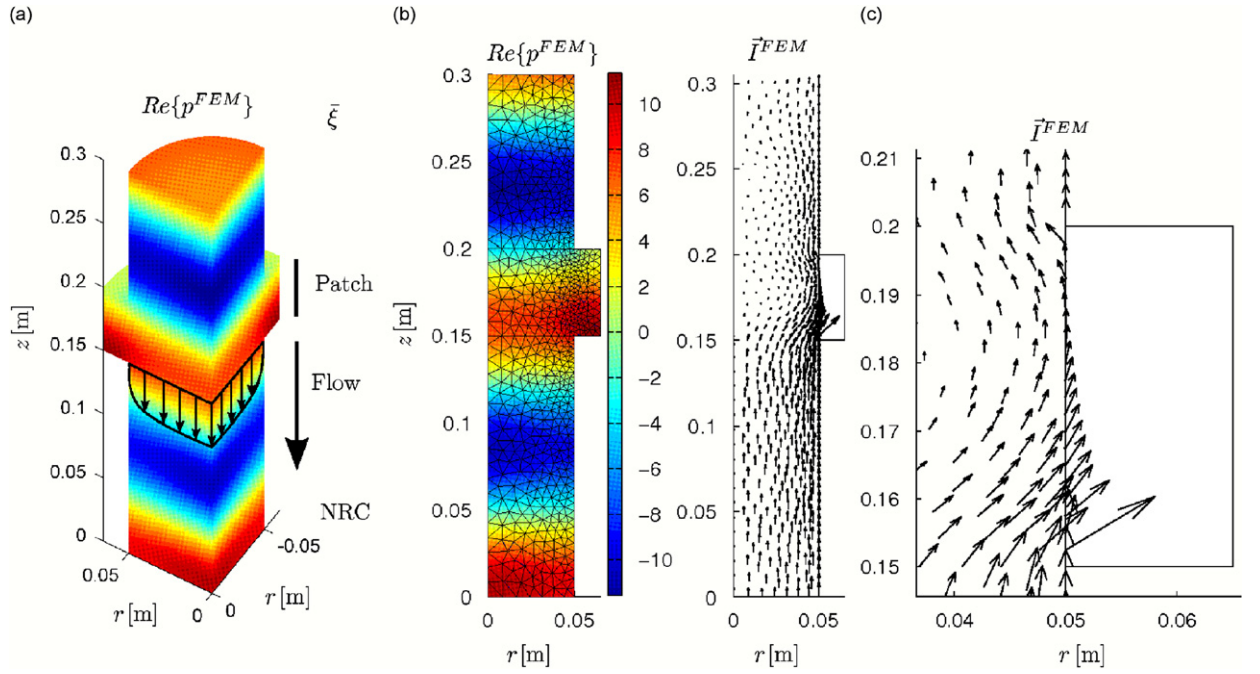

Fig. 25. (a) Pressure field. (b) Pressure and intensity field in a cross section. (c) Zoom on intensity field.

governed by Biot's model and Galbrun's equation. Galbrun's equation is a reformulation of the Linearized Euler's Equations written in terms of the Lagrangian perturbation of Eulerian variables. With this Lagrangian representation, an exact expression for the energy flux and acoustic intensity can be found and can supply a good tool for studying absorbing material with sheared mean flow (see Fig. 25).

Here, the coupling between Galbrun's and Biot's equation is realized with mixed pressure-displacement FE. On the one hand, mixed formulation is used in Galbrun's equation to avoid numerical locking [34]. And on the other hand, in poroelastic media, the description of both phases involves the displacement of the solid phase and the pressure in the fluid phase [35]. The method has been validated with analytical results, for more details see Ref. [36].

Written by Benoit Nennig, Mabrouk Ben Tahar, Emmanuel Perrey-Debain, benoit.nennig@utc.fr, Université de Technologie de Compiègne, France.

5.6. Computation of aeroacoustic phenomena in subsonic and transonic ducted flows

Strong interactions between shock oscillations, internal aerodynamic noise and acoustic duct modes, often observed in confined flows, are usually undesirable in view of vibrations and fatigue of structures. In order to compute this kind of phenomena, a numerical solver called Simulation of Aeroacoustics in Fluids And Resonance and Interactions (SAFARI) has been developed. Compressible Navier–Stokes equations are solved using high-order finite difference schemes [38]. A transonic flow passing a sudden expansion in a duct is studied [39]. Strong coupling between the self-sustained oscillations of the normal shock and the longitudinal acoustic modes is captured as in the experiments. An instantaneous snapshot of the density gradient modulus is represented in Fig. 26. For lower pressure ratios, the flow is entirely supersonic with oblique shocks. For higher pressure ratios, the flow is asymmetric and exhibits shock cells.

Written by Philippe Lafon, philippe.lafon@edf.fr, Electricité de France, France.

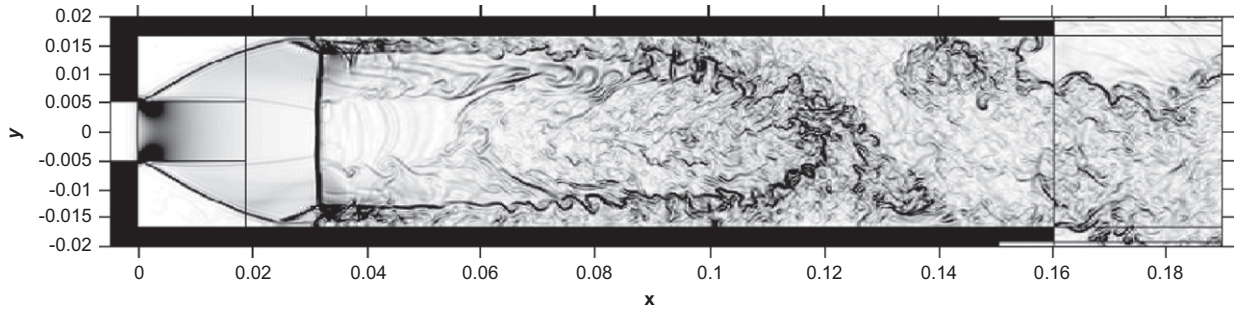

Fig. 26. Instantaneous snapshot of the modulus of the density gradient. The duct walls are represented in black.

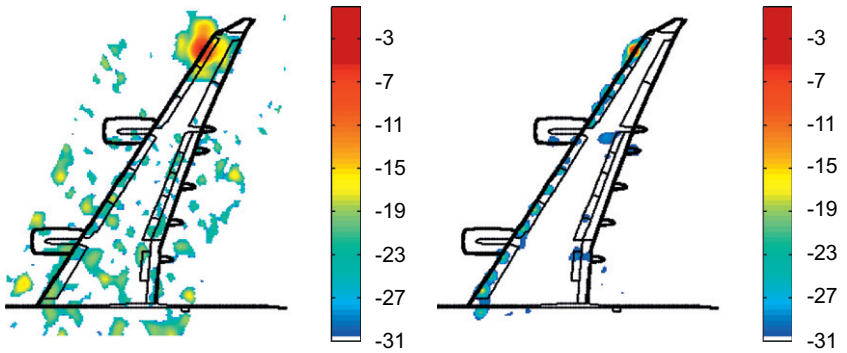

Fig. 27. Source plots obtained with conventional beamforming (left) and CLEAN-SC (right).

5.7. *Phased array deconvolution using CLEAN-SC*

A new phased array deconvolution technique, developed at NLR, takes advantage of the fact that sources in source plots are spatially coherent with their side lobes. Beam patterns of individual noise sources are determined by analyzing the measured spatial coherence. This avoids the use of Point Spread Functions (PSFs), which are obtained by synthesizing data of monopole point sources. Traditionally, deconvolution methods assume that source maps are built up by PSFs, which may lead to errors when actual source patterns are different. The new method is called *CLEAN based on Source Coherence* (CLEAN-SC), as it is a modified version of the classical CLEAN method used in Astronomy. Essentially, CLEAN-SC iteratively removes the part of the source plot which is spatially coherent with the peak source. A feature of CLEAN-SC is its ability to extract absolute sound power levels from the source plots. The merits of CLEAN-SC were demonstrated using array measurements of airframe noise on a scale model of the Airbus A340 (Fig. 27) in the $8 \times 6\,\mathrm{m}^2$ closed test section of DNW-LLF, carried out in the EU-project AWIATOR. For details, see Ref. [40].

Written by Pieter Sijtsma, sijtsma@nlr.nl, NLR, The Netherlands.

5.8. *Localization and tracking of aircraft with ground based 3D sound probes*

Traditional acoustic far-field sound source localization measurements are based on arrays of sound pressure transducers [41,42]. These techniques have technical and practical limitations and rely on assumptions that are not always justified. An alternative localization and tracking method is demonstrated [43] which is based on a pair of three-dimensional sound intensity probes. These compact and broad-banded 3D sound probes are based on three (orthogonal) velocity sensors and a sound pressure transducer, to provide acoustic-vector information over the entire audio range [44]. A series of three tests with increasing complexity was carried out to demonstrate the principle: (i) anechoic room experiments to reconstruct a stationary source at different

positions; (ii) outdoor experiments with a moving sound source (walking speed); (iii) experiments tracking a moving helicopter (during take-off and landing), by using the blade-passage frequency of the main rotor for detection (see Fig. 28).

Written by Alex Koers, koers@microflown.com, Microflown Technologies, The Netherlands.

5.9. Non-destructive and in-situ acoustic testing of inhomogeneous materials

The so-called PU surface impedance method was first introduced in 2004. This free field method, based on the measurement of both sound pressure and particle velocity at the surface, is fast, requires only small sample sizes and no anechoic room. Applicability of the method, proven for soft-porous homogenous materials [45–47], has been extended to include inhomogeneous aerospace materials of relatively complex geometry. It has been shown [48] that the PU surface impedance method can be applied to determine impedance, reflection and absorption of inhomogeneous materials in high spatial resolution, viz. on the scale of few millimeters. Particle velocity levels of large dynamic range yield measuring local impedance distributions with high spatial resolution. A range of local measurements on a hollow sphere of aluminum foam material could reconstruct the overall average impedance and absorption values, obtained with a Kundts tube (see Fig. 29).

Written by Alex Koers, koers@microflown.com, Microflown Technologies, The Netherlands.

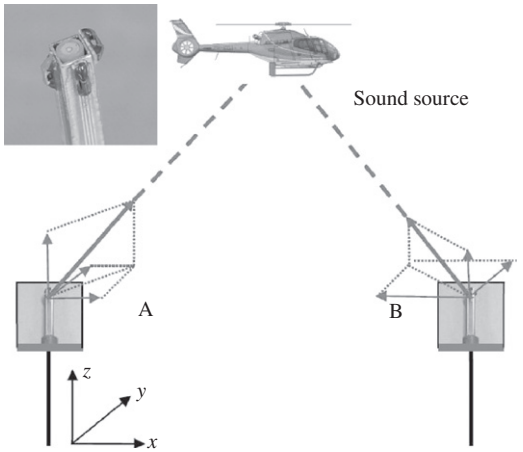

Fig. 28. Two 3D sound probes to track sound source location; close up of 3D sound probe.

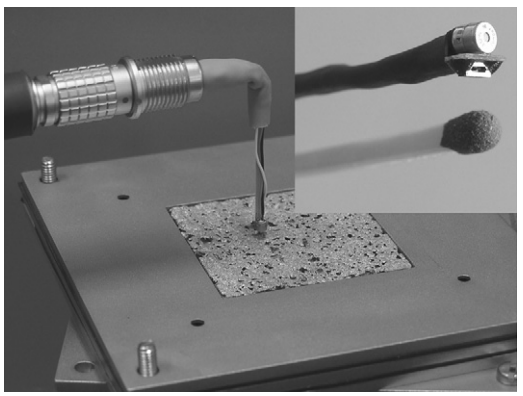

Fig. 29. Local PU surface impedance measurements on aluminum foam, close up PU match probe.

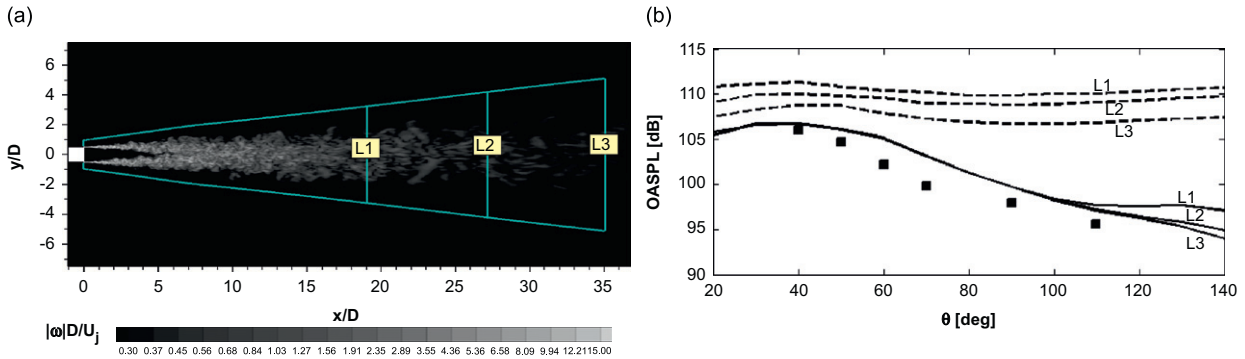

Fig. 30. (a) LES turbulent jet simulation showing three different lengths of FWH surface; x, y, are co-ordinates, D is jet diameter, U_j is jet velocity. Contours show instantaneous vorticity magnitude $|\omega|$ in scaled non-dimensional form. Jet/co-flow Mach numbers 0.77, 0.26; stagnation temperature ratio 2.66; acoustic Mach number 1.26. (b) Overall sound pressure level vs. angle from jet axis θ at radius $100D$, according to: measurements [51] (□); LES + wave extrapolation (WE), using standard FWH based on density (- - - -); WE using modified FWH based on pressure [50] (——).

5.10. Improved jet noise extrapolation

Ffowcs Williams & Hawkings (FWH) surfaces (''sleeves'') are often used to extrapolate the sound from jet simulations (LES or DNS) to the acoustic far field. Downstream closure of the sleeve presents a problem with the standard formulation (based on density): when entropy variations in a hot jet cross the FWH surface, the standard formulation leads to an unrealistically large surface-term contribution [49]. Ideally this contribution would be cancelled by volume terms outside the surface, but the neglect of volume terms is inherent to the wave extrapolation process. In Ref. [50] a modified FWH formulation is developed, based on pressure, that nearly eliminates the closure problem and formalises a heuristic proposal made by Shur et al. [49]. Fig. 30 compares the two formulations for LES of a hot subsonic jet in co-flow corresponding to the measurements of [51], using various sleeve lengths. The benefit of the new formulation is obvious.

The computations were performed at New Technologies and Services.

Written by M.L. Shur, New Technologies and Services, St. Petersburg, Russia, P.R. Spalart, Boeing Commercial Airplanes, M.C.M. Wright and C.L. Morfey, ISVR, University of Southampton, UK, clm@isvr.soton.ac.uk.

5.11. High resolution shock-capturing LES methods for CAA of compressible, turbulent flows

A recent analysis of the dissipation of kinetic energy in Godunov schemes [52] has led to the development of new very high-order (ninth-order) accurate numerical methods, which are both shock capturing and capable of resolving low Mach, turbulent flow features [74]. As the methods are fully compressible, and are not based on an expansion of the Euler equations at low Mach numbers, then acoustic waves are represented accurately. The new methods have been validated through simulation of compressible turbulent flow over a deep, open cavity [53]. Results shown in Fig. 31 demonstrate that the frequency of the fundamental mode is captured to within 1% accuracy, and the amplitude to within 2 dB.

Written by D. Drikakis, d.drikakis@cranfield.ac.uk, Cranfield University, UK.

5.12. Advances in emission surface algorithms

In the framework of EU project Friendcopter an aeroacoustic prediction tool was developed based on the coupling of acoustic analogy and CFD. The work focuses on the development of a porous emission surface algorithm for tackling the problem of high-speed impulsive (HSI) noise generated by transonic and supersonic rotating sources. To date, the emission surface formulation has not been extensively used because of numerical/mathematical difficulties associated with the construction of integration surface. The most well-known approaches are the marching cubes algorithm [54] and the porous version of the

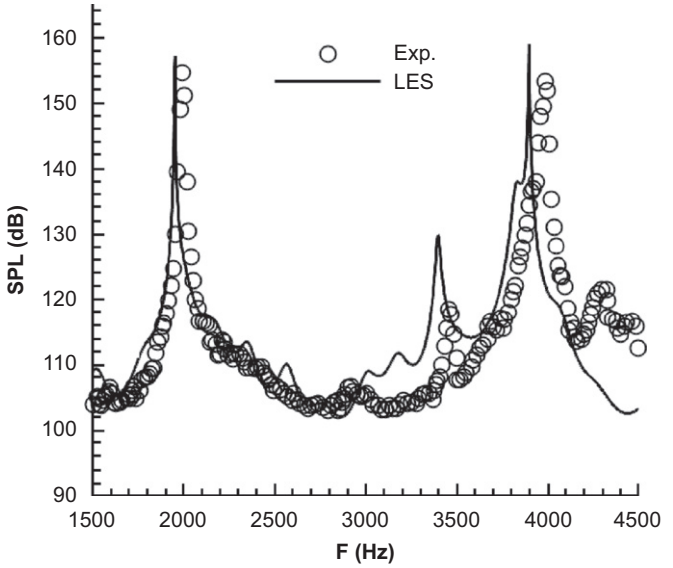

Fig. 31. Sound pressure levels within the cavity compared to the experimental results of Forestier et al. [53].

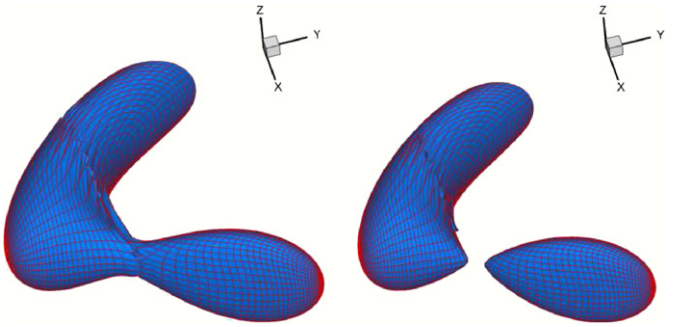

Fig. 32. Emission surface at different times for a sphere of 0.5 m radius centered at (0,1,0) and rotating around the z-axis with speed of 600 rad/s. The observer is located at $x = (3,0,0)$.

k-algorithm [55]. Instead, a new approach is considered here based on the retarded time equation and application of Taylor series expansion for obtaining the sources distribution and emission time. Indicatively, Fig. 32 shows the results obtained with the new approach for the emission surface for a sphere rotating at speeds ranging from Mach 0.7 to 1.5.

Written by D. Drikakis, d.drikakis@cranfield.ac.uk, Cranfield University, UK.

5.13. Impedance modeling of acoustic panels in presence of grazing flow

The effective impedance of liners with grazing flow has been studied by CFD models for the interaction between sound and the perforate facing sheet surface of typical acoustic panels (see an example in Fig. 33). Flow data are then post-processed in order to extract surface impedance. Results are finally compared with measured impedance obtained by in-situ impedance measurements of panels tested in the NLR Flow Duct Facility [56].

Written by P. Ferrante, piergiorgio.ferrante@aermacchi.it, AleniaAermacchi, Italy.

5.14. Turbofan Aft noise predictions based on the Lilley's wave model

Lilley's equation, discretized in frequency domain by using the GFD method [57,58], has been solved to compute the sound radiated from an aero-engine by-pass duct model, for which an analytical solution is

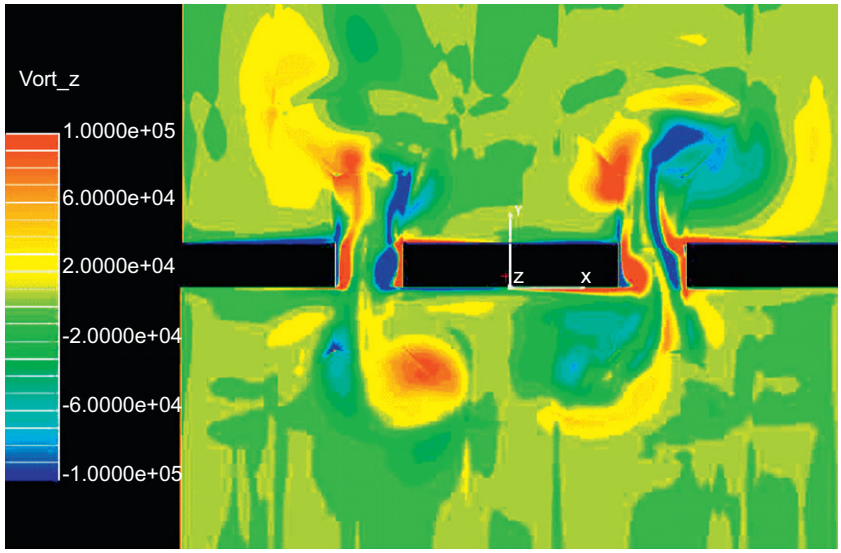

Fig. 33. Vorticity generated by sound plane wave incident on a perforate acoustic panel (CFD computation).

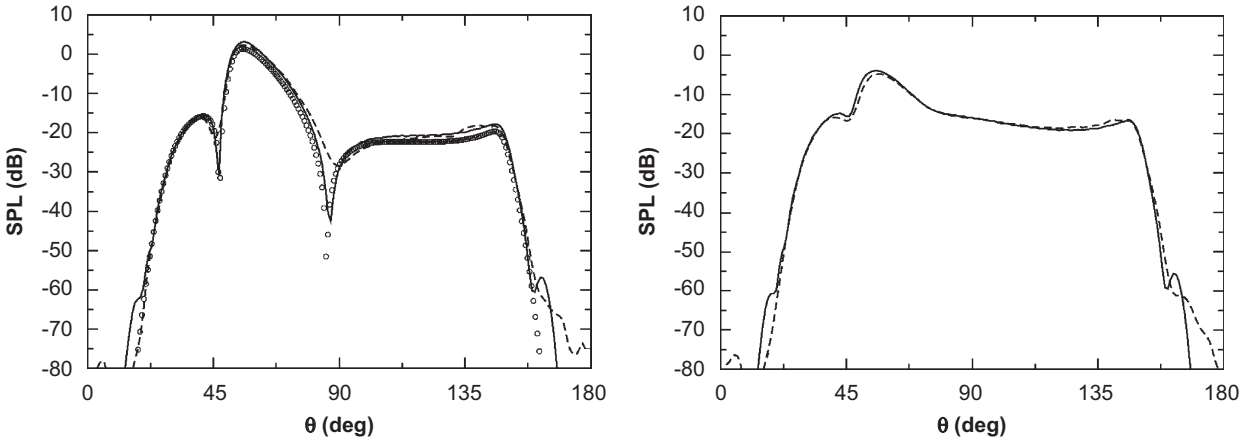

Fig. 34. By-pass sound directivity. Free-stream Mach number 0.25, by-pass Mach number 0.45, Helmholtz number 30, cut-on ratio 1411, mode (17,2). Hard wall afterbody on the left, acoustically treated afterbody on the right ($Z = 2-i$). Comparison between analytical (symbols), 2.5D GFD results (solid line), and 3D GFD results (dashed line).

available. Both axi-symmetric (2.5D) and 3D simulations have been carried out [57]. A novel PML approach for annular buffers has been developed for the 3D simulations [57], whereas an ad-hoc edge treatment has been employed [58]. Fig. 34 shows a comparison between the numerical and analytical sound directivities. A favorable agreement can be observed between the analytical and the 2.5D GFD solutions, as well as between the 2.5D and 3D GFD solutions, even though the latter one was obtained by using a quite coarser mesh. A further step towards a more realistic simulation has been accomplished by considering the by-pass duct configuration of Fig. 35 for which the mean flow has been computed by using Fluent^{TM}. The spinning mode (52, 1) is propagated from the bypass inlet plane through the duct and radiated into the far-field. The acoustic frequency is such that the Helmholtz number based on the bypass inlet external radius is 110.

Written by D. Casalino, d.casalino@cira.it, CIRA, Italy.

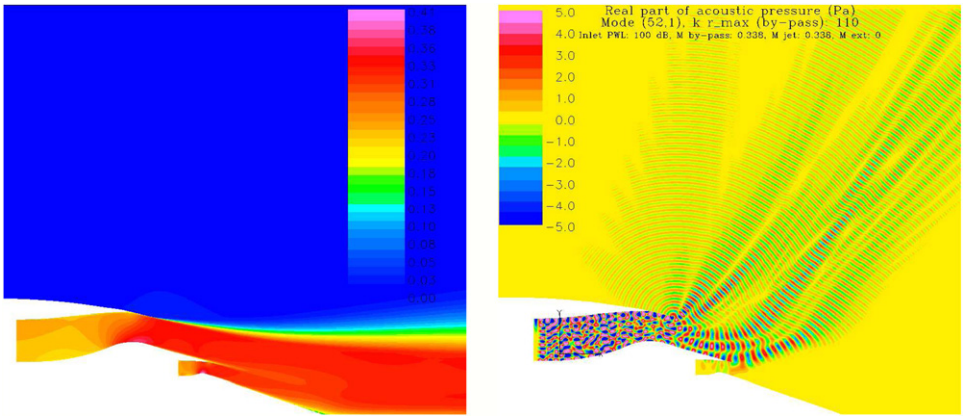

Fig. 35. Sound radiation from a realistic by-pass configuration. Dimensionless velocity field on the left, acoustic field on the right. Free-stream Mach number 0, by-pass and jet Mach numbers 0.338, Helmholtz number 110, mode (52,1).

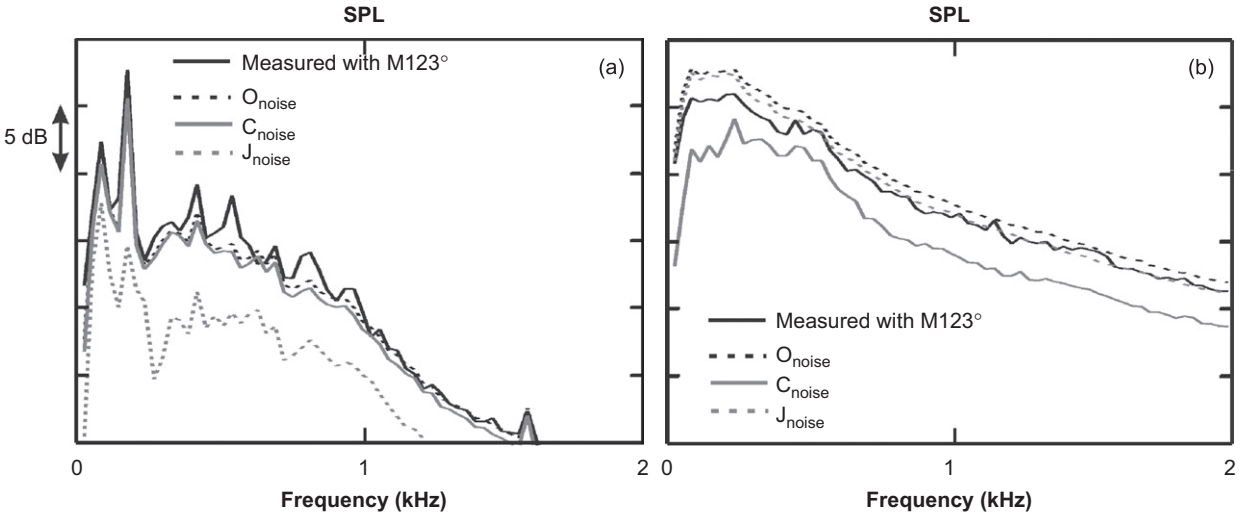

Fig. 36. Contribution of combustion noise C_{noise}, jet noise J_{noise} and C_{noise} plus J_{noise} computed with SEM, compared with the measured spectrum with M_{123°. (a) Results at low operating condition and (b) results at high operating condition.

5.15. *Separation of combustion and jet noise of a turbofan engine with SEM method*

A full-scale test on a turbofan engine has been carried out on the open-air test facility 4D of General Electric located at Peebles (Ohio), in the framework of the European SILENCE(R) project (Section 2.1). One of the primary objectives of the experiment managed by SNECMA was to discriminate combustion noise from the jet noise using data measured in the near-field with an array of microphones and the so-called Spectral Estimation Method (SEM). An illustration of the procedure of separation made with SEM [59] is shown in Fig. 36. Comparisons between SEM spectra C_{noise}, J_{noise} and O_{noise}, respectively, due to the emission regions of combustion noise, jet noise, and of the sum of combustion plus jet noise, and measured downstream with a microphone named M_{123°, at the angular location of 123° where the combustion noise is dominant are presented. At low operating condition, combustion noise is dominant, and we have the spectrum measured with M_{123° and C_{noise} which are in agreement (Fig. 36a). In contrast, the contribution of jet noise is weaker compared to C_{noise}, while O_{noise} matches well with the spectrum measured with M_{123°. At high operating

condition, the dominant source is jet noise as shown in Fig. 36b. Its level is comparable with that measured with M_{123°. In contrast, combustion noise is approximately 3 dB weaker than the measured spectrum and of O_{noise} and J_{noise}.

Written by Daniel Blacodon, Daniel.Blacodon@onera.fr, ONERA, France.

6. Miscellaneous topics

6.1. Reduction of the sonic boom from a high-speed train entering a gallery

A train passing through a tunnel generates pressure waves that propagate back and forth to the portals where they are reflected. The combination of these waves with the motion of the train generates a very complex flow pattern where the transient pressure can affect the passenger comfort and safety and cause damages to train parts. Several measures either on the trains or on the tunnels need to be used to alleviate the most severe pressure effects. A 1:87 scaled-model experimental facility has been designed and used for analyzing and comparing different configurations (train noses, tunnel entrances, airshafts, etc.). It has been shown that replacing an abrupt entrance by a progressive one has beneficial effects on the gradient of the compression wave. A less costly civil engineering construction would be to construct airshafts along the tunnel. Several distributions have been tested, among which one proposed by Howe. Optimizing the geometry and positioning of airshafts could alleviate the pressure rise in a significant way and reduce the pressure gradient up to a factor 6 (Fig. 37). Details can be found in Anthoine et al. [60].

Written by J. Anthoine, anthoine@vki.ac.be, VKI, Belgium.

6.2. Combustion noise investigations using APE-RF and different sound source formulations

Combustion noise and sound source mechanisms of an unconfined turbulent non-premixed flame is investigated. A hybrid LES/CAA approach is employed in which a low Mach number variable density large-eddy simulation (LES) is combined with the acoustic perturbation equations for reacting flows. In the first step of the hybrid analysis the flamelet/progress variable [61] model is employed as combustion model followed by the acoustic simulation. In the second step using the acoustic perturbation equations for reacting flows [62].

The flamelet/progress variable database has been extended in terms of acoustic source terms. The unsteady heat release rate, the source describing the effect of non-isomolar combustion, and the species diffusion term are described by two independent parameters, i.e., the mixture fraction and the progress variable. From the findings in the present study, the analysis of the acoustic field of low Mach number reacting flows induced by the thermoacoustic sources such as the unsteady heat release leads to a very stiff problem formulation,

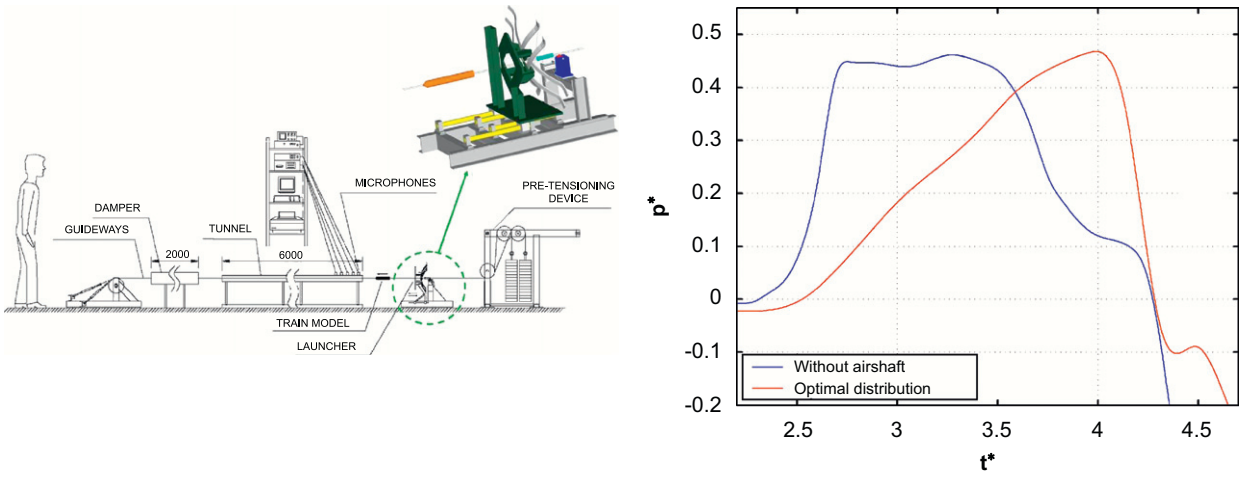

Fig. 37. Experimental facility (left) and comparison of the pressure pattern without airshaft and with the optimal distribution of airshafts.

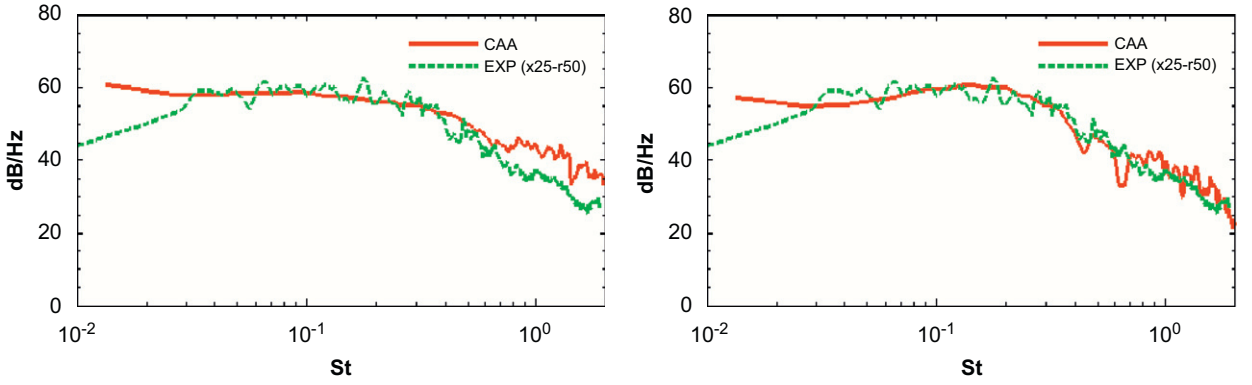

Fig. 38. Spectra in the frequency range of $0.01 < \mathrm{St.} < 2$ are shown. Comparison of measured and computed sound spectra level at $r/D = 50$ and $x/D = 25$ using the scaled substantial time derivative of the density (left) or the scaled partial time derivative of the density (right) as simplified source formulation.

since the related sources require highly resolved regions in the source area, which restricts the possible time step during temporal integration of the equations. The numerical bottleneck is not so restrictive when a source term formulation based on the density distribution is used. Spectra obtained from the simulated acoustic field, using two different source term formulations involving derivatives of the density are in good agreement with the experimental data even in the higher frequency range (see Fig. 38).

Written by T. Ph. Bui, W. Schröder, and M. Meinke, p.bui@aia.rwth-aachen.de, RWTH Aachen University, Germany.

6.3. Acoustically optimized approach and departure procedures

Contrary to technological noise reduction methods for aircraft, noise abatement flight procedures can be used also for existing aircraft and thus make short- or mid-term noise reductions in the environment of airports feasible. An optimization of flight procedures for transport aircraft was carried out, based on a prediction method and subsequent experimental validation involving the following steps: (1) physical description of all relevant sound sources of transport aircraft; (2) empirical prediction of noise contours during departure and approach; (3) simulation of different approach and departure procedures to identify acoustically optimized procedures and their effect on the airport capacity; investigation of potentially increased work load of pilots, and (4) experimental verification of predicted noise reduction potential of noise abatement flight procedures by means of flight tests. Promising low noise variants of low-drag-low-power (LDLP) approach procedures were developed [63] off-line for an A319 aircraft on the basis of DLR's models for engine [64] and airframe [65] noise prediction. The noise impact of different flight procedures was investigated by means of ground microphone measurements during an extensive flight test campaign with an A319 aircraft, supplied and operated by Deutsche Lufthansa on the Baltic Airport in North-Germany.

A noise reduction potential of on average 1–3 dB was shown to exist for the approach procedures, with higher local reductions occurring at larger distances from the airport, see Fig. 39. For departure procedures, reductions are limited to about 1 dB. With suitable flight management systems, the new flight procedures are not critical from a pilot's work load point of view. For more information see the final report [66] (in German). This German national research project was carried out by Deutsche Lufthansa, EADS-IW, Deutsche Flugsicherung, TU Braunschweig, and DLR.

Written by W. Neise, M. Pott-Pollenske, R. König, U. Isermann, and S. Guérin, michael.pott-pollenske@dlr.de, DLR, Germany.

6.4. Aeroacoustics and MDO

The inclusion of aeroacoustic-related objectives and constraints in a multidisciplinary design optimization (MDO) environment is one of the exciting developments for the next generation design tools.

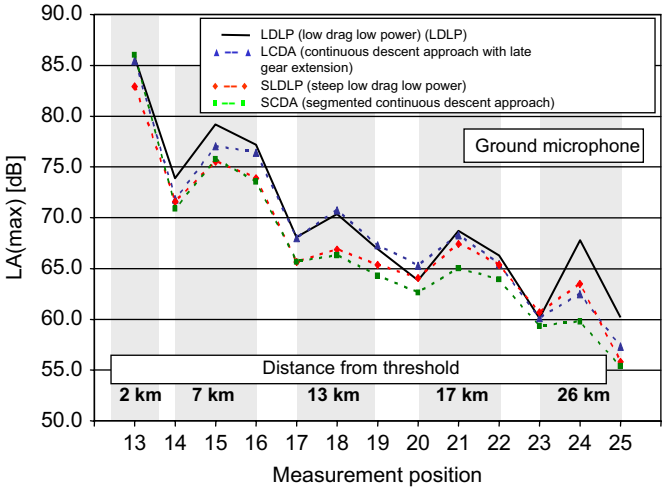

Fig. 39. Comparison of measured maximum A-weighted sound pressure levels for different noise abatement procedures.

The optimization environment framework for innovative design in aeronautics (FRIDA), developed at the University Roma Tre, has been recently enriched by new simulation modules, dedicated to the evaluation of the community noise impact of commercial aircraft. Further to the classical sound-level-based approach, an innovative technique has been developed to introduce sound-quality issues in the design. The method is based on the measure of the difference between the acoustic emissions in specific operation conditions, and a given target sound. This original approach has been developed within the context of the EC funded project SEFA (Section 2.2). Additional activities, closely related to the same topic, are the development of algorithms for the treatment of variables known only on statistical basis, and the inclusion of multi-fidelity models management schemes, both aimed at a robust and efficient optimal design of highly innovative, environmental-friendly configurations [67–69].

Written by Umberto Iemma and Matteo Diez, u.iemma@uniroma3.it, University Roma Tre, Italy.

6.5. Plasma actuation for noise control

A new activity was initiated at Southampton University to develop atmospheric pressure plasma actuators to reduce aerodynamic noise. Plasma actuators do not have any mechanical moving parts, which makes them simple and reliable. The principle of using plasma actuators for aerodynamic noise control is to alter the airflow around an object through interaction between flow and electric fields, thus affecting the sound field (without the need to physically change the shape of the object). The method proved to be successful in attenuating noise radation from a cavity [70] by producing spanwise velocity variations in the shear layer (Fig. 40). In addition, the driving signal of plasma actuators was optimized [71], and a closed-loop control method was proposed [72] to increase power efficiency by up to 200%. The actuators are now being applied to several bluff bodies for broadband noise control.

Written by X. Huang and X. Zhang, x.zhang1@soton.ac.uk, University of Southampton, UK.

7. Propeller noise

7.1. Spectral decomposition in noise abatement of propeller airplanes

High-resolution spectral analysis and decomposition can be a very effective tool in noise analysis and abatement of propeller airplanes. It requires no special measuring instrumentation and can be very fast. A software stool called spectral analysis and decomposition (SPAD) has been developed for fast analysis of turboprop airplane noise. The basic code computes continuously short-time high-resolution spectra in which it traces salient discrete spectral components. Next, it finds and allocates the components, caused by a specific

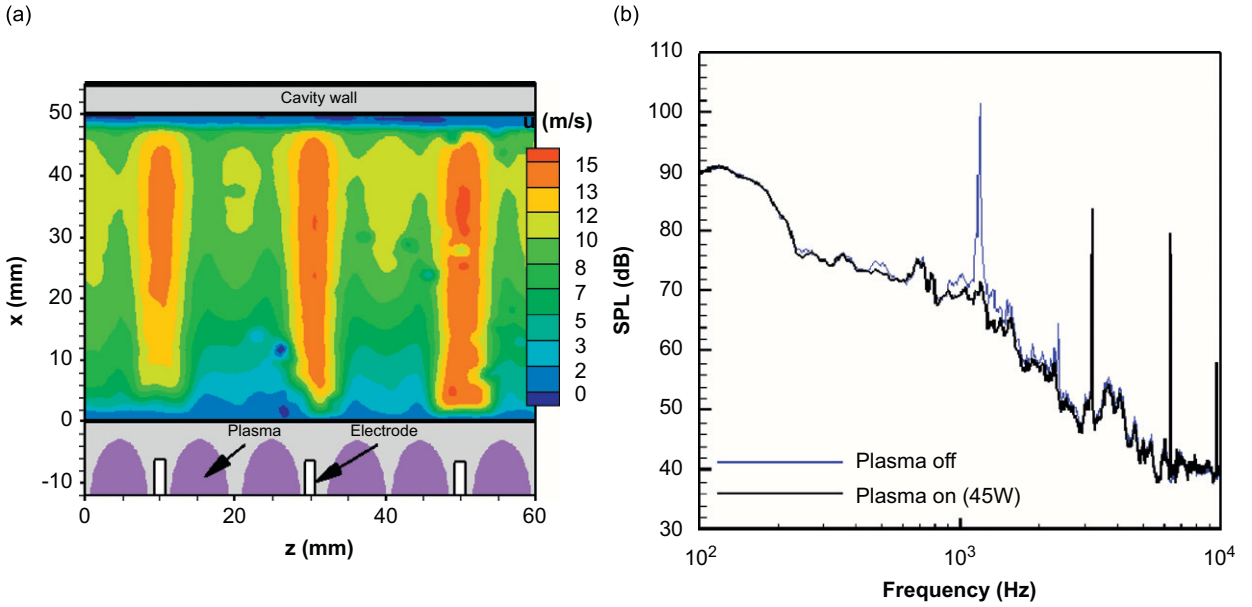

Fig. 40. (a) Streamwise mean velocity variation of the shear layer spanning a cavity and (b) sound level reduction. $U_\infty = 20\,\mathrm{m/s}$. Flow from bottom to top. Plasma actuators operating with 15 kV (peak-to-peak voltage) and 45 W.

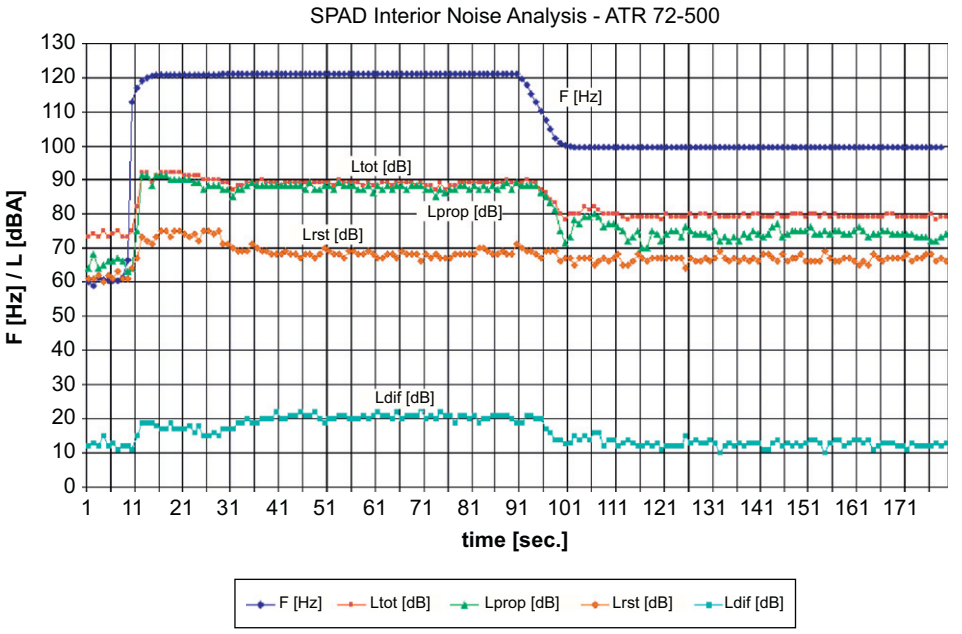

Fig. 41. An example of the SPAD analysis of a 3 min record of the noise in a turbo propeller airplane during its take-off and climbing on full and reduced power of the engines.

cyclic processes. Finally it decomposes the found harmonic spectral components and determines the characterizing quantities, like fundamental frequency (F_1[Hz]), overall sound pressure level (L_{tot} [dB]), etc. An example is shown in Fig. 41. Analyzed has been a 3 min long calibrated record of the interior noise in a turbo propeller aircraft during its take off run, full power climbing, and transition to climbing with reduced power of the engines [73].

Written by Tomas Salava, salava@vzlu.cz, Aeronautical Test and Research Institute, Czech Republic.

References

[1] G.A. Gerolymos, D. Sénéchal, I. Vallet, Pressure, density and temperature fluctuations in subsonic flows and broadband noise, AIAA Paper 2007-3408, *13th AIAA/CEAS Aeroacoustics Conference*, Roma, Italy, 21–23 May, 2007.

[2] B. Greschner, S. Peth, Y.J. Moon, J.H. Seo, M.C. Jacob, F. Thiele, Three-dimensional predictions of rod wake-airfoil interaction noise by hybrid methods, *Proceedings of the 14th International Congress on Sound and Vibration*, Cairns, Australia, 9–12 July, 2007.

[3] M.C. Jacob, J. Grilliat, R. Camussi, G. Caputi Gennaro, Experimental study of a tip leakage flow—part one: aerodynamic and acoustic measurements, AIAA paper 2007-3684, *13th AIAA/CEAS Aeroacoustics Conference*, Roma, Italy, May 21–23, 2007.

[4] R. Camussi, G. Caputi Gennaro, M.C. Jacob, J. Grilliat, Experimental study of a tip leakage flow—part two: wavelet analysis of wall pressure fluctuations, AIAA paper 2007-3685, *13th AIAA/CEAS Aeroacoustics Conference*, Rome, Italy, May 21–23, 2007.

[5] V. Jurdic, A. Moreau, P. Joseph, L. Enghardt, J. Coupland, A comparison between measured and predicted fan broadband noise due to rotor-stator interaction, AIAA paper 2007-3692, *13th AIAA/CEAS Aeroacoustics Conference*, Rome, Italy, May 21–23.

[6] P. Sijtsma, Feasibility of in-duct beamforming, AIAA paper 2007-3696, *13th AIAA/CEAS Aeroacoustics Conference*, Rome, Italy, May 21–23, 2007.

[7] J.E. Ffowcs Williams, L.H. Hall, Aerodynamic sound generation by turbulent flow in the vicinity of a scattering half-plane, *Journal of Fluid Mechanics* 40 (4) (1970) 657–670.

[8] M. Herr, A noise reduction study on flow-permeable trailing-edges, *Conference Proceedings of the Eighth ONERA-DLR Aerospace Symposium* (*ODAS*), 17–19 October, Göttingen, Germany, 2007.

[9] T.F. Brooks, D.S. Pope, M.A. Marcolini, Airfoil Self-Noise and Prediction, NASA Reference Publication 1218, 1989.

[10] P. Moriarty, *NAFNoise User's Guide*, National Wind Technology Centre, National Renewable Energy Laboratory, Golden, CO, July 2005 URL: 〈http://wind.nrel.gov/designcodes/simulators/NAFNoise〉.

[11] R. Ewert, Broadband slat noise prediction based on CAA and stochastic sound sources from a fast random particle-mesh (RPM) method, *Computers & Fluids* 37 (4) (2008) 369–387.

[12] G. Scarselli, L. Lecce, F. Amoroso, K. Janssens, A. Vecchio, Numerical simulation, experimental comparison with noise measurements and sound synthesis of airframe noise, *13th AIAA/CEAS Aeroacoustics Conference*, Rome, Italy, May 2007.

[13] J. Yan, K. Tawackolian, U. Michel, F. Thiele, Computation of jet noise using a hybrid approach. AIAA Paper 2007-3621. *13th AIAA/CEAS Aeroacoustics Conference*, Rome, Italy, May 2007.

[14] J. Yan, L. Panek, F. Thiele, Simulation of jet noise from a long-cowl nozzle with serrations. AIAA Paper 2007-3635, *13th AIAA/CEAS Aeroacoustics Conference*, Rome, Italy, May 2007.

[15] J. Bridges, C. Brown, Parametric testing of chevrons on single flow hot jets, *10th AIAA/CEAS Aeroacoustics Conference*, Manchester, UK, Paper No. AIAA-2004-2824, 2004.

[16] S. Redonnet, E. Manoha, P. Sagaut, Numerical simulation of propagation of small perturbations interacting with flows and solid bodies, AIAA Paper nr. 2001-2223, *Seventh CEAS/AIAA Aeroacoustics Conference*, Maastricht, The Netherlands, 28–30 May 2001.

[17] M. Terracol, E. Labourasse, E. Manoha, P. Sagaut, Simulation of the 3D unsteady flow in a slat cove for noise prediction, AIAA Paper no. 2003-3110, *Ninth AIAA/CEAS Aeroacoustics Conference*, Hilton Head, USA, 12–14 May, 2003.

[18] S. Redonnet, G. Desquesnes, E. Manoha, M. Terracol, Numerical study of acoustic installation effects through a chimera CAA method, AIAA-2007-3501, *13th AIAA/CEAS Aeroacoustics Conference*, Rome, Italy, May 21–23, 2007.

[19] T. Castelain, M. Sunyach, D. Juvé, J.C. Béra, Jet-noise reduction by impinging microjets: an acoustic investigation testing microjets parameters, *AIAA Journal* 46 (5) (2008) 1081–1087.

[20] T. Castelain, Contrôle de jet par microjets impactants. Mesure de bruit rayonné et analyse aérodynamique, PhD Thesis, ECL-No. 2006-33, 2006.

[21] G. Perez, J. Prieur, G. Rahier, F. Vuillot, Theoretical and numerical discussion on volume integral methods for jet noise prediction, AIAA paper 2007-3593, *13th AIAA/CEAS Aeroacoustics Conference*, Roma, Italy, 21–23 May 2007.

[22] F. Vuillot, N. Lupoglazoff, N. Rahier, Double-stream nozzles flow and noise computations and comparisons to experiments, *46th AIAA Aerospace Sciences Meeting and Exhibit*, Reno, USA, 7–10 January 2008.

[23] W. De Roeck, Hybrid Methodologies for the Computational Aeroacoustic Analysis of Confined Subsonic Flows, PhD Thesis, K.U. Leuven, Belgium, 2007.

[24] G. Rubio, W. De Roeck, M. Baelmans, W. Desmet, Large Eddy simulation for computation of aeroacoustic sources in 2D-expansion chambers, in: Eric Lamballais, Rainer Friedrich, Bernard J. Geurts, Olivier Metais (Eds.), Direct and Large-Eddy Simulation VI, 2006, pp. 555–564.

[25] G. Rubio, W. De Roeck, J. Meyers, M. Baelmans, W. Desmet, Aeroacoustic noise source mechanisms in simple expansion chambers, AIAA-paper 2006-2700, 2006.

[26] W. De Roeck, G. Rubio, W. Desmet, On the use of filtering techniques for hybdrid methods in computational aero-acoustics, *International Conference on Sound and Vibration*, ISMA 2006, Leuven, Belgium, 2006.

[27] W. De Roeck, M. Baelmans, W. Desmet, Aerodynamic/acoustic splitting technique for computation aeroacoustics applications at low Mach numbers, *AIAA Journal* 46 (2008) 463–475.

[28] J. Christophe, P. Rambaud, J. Anthoine, C. Schram, F. Mathey, S. Moreau, Prediction of incoming turbulent noise using a combined numerical/semi-empirical method and experimental validation, AIAA-2007-3468, *13th AIAA/CEAS Aeroacoustics Conference*, Rome, Italy, 21–23 May 2007.

[29] C.K.W. Tam, L. Auriault, Jet mixing noise from fine-scale turbulence, *AIAA Journal* 37 (2) (1999).

[30] R. Ewert, RPM—the fast Random Particle-Mesh (RPM) method to realize unsteady turbulent sound sources and velocity fields for CAA applications, AIAA Paper 2007-3506, 2007.
[31] C.K.W. Tam, K. Viswanathan, K.K. Ahuja, J. Panda, The sources of Jet Noise: Experimental Evidence, AIAA Paper 2007-3641, 2007.
[32] F. Lörcher, G. Gassner, C.-D. Munz, A Discontinuous Galerkin scheme based on a space-time expansion. I. Inviscid compressible flow in one space dimension, *Journal of Scientific Computing* 32 (2007) 175–199.
[33] G. Gassner, F. Lörcher, C.-D. Munz, A discontinuous Galerkin scheme based on a space-time expansion. II. Viscous compressible flow in multi space dimensions, *Journal of Scientific Computing* 34 (2008) 260–286.
[34] F. Treyssède, G. Gabard, M. Ben Tahar, A mixed finite element method for acoustic wave propagation in moving fluids based on an eulerian lagrangian description, *Journal of the Acoustic Society of America* 113 (2) (2003) 705–716.
[35] N. Atalla, M.A. Hamdi, R. Panneton, Enhanced weak integral formulation for the mixed (u, p) poroelastic equations, *Acoustic Society of America* 109 (6) (2001) 3065–3068.
[36] B. Nennig, M. Ben Tahar, E. Perrey-Debain, A 3D numerical method for studying poroelastic liners with mean flow, *Proceedings of ICSV14*, Cairns, Australia, July 9–12, 2007.
[38] C. Bogey, C. Bailly, D. Juvé, A family of low dispersive and low dissipative schemes for Large Eddy Simulations and for sound propagation, *Journal of Computational Physics* 194 (2004) 194–214.
[39] T. Emmert, P. Lafon, C. Bailly, Computation of aeroacoustic phenomena in subsonic and transonic ducted flows, AIAA 2007-3429, *13th AIAA/CEAS Aeroacoustics Conference*, Rome, Italy, 2007.
[40] P. Sijtsma, CLEAN based on spatial source coherence, *International Journal of Aeroacoustics* 6 (4) (2007) 357–374.
[41] B.G. Ferguson, A ground-based narrow band passive acoustic technique for estimating the altitude and speed of a propeller driven aircraft, *Journal of the Acoustical Society of America* 92 (3) (1992) 1403–1407.
[42] N. Roosnek, Passive ranging with four microphones in a spatial configuration, *Internoise 2001*, The Hague, The Netherlands, 2001.
[43] T.G.H. Basten, H.-E. De Bree, E.H.G. Tijs, Localization and tracking of aircraft with ground-based 3D sound probes, Paper presented at the *33rd European Rotorcraft Forum*, Kazan, Russia, 11 September 2007.
[44] F. Jacobson, H.-E. De Bree, A comparison of two different sound intensity measurement principles, *Journal of the Acoustical Society of America* 118 (3) (2005) 1510–1517.
[45] R. Lanoye, G. Vermeir, W. Lauriks, R. Kruse, V. Mellert, Measuring the free field acoustic impedance and absorption coefficient of sound absorbing materials with a combined particle velocity-pressure sensor, *JASA*, May 2006.
[46] H.-E. De Bree, R. Lanoye, S. De Cock, J. Van Heck, Broad band method to determine the normal and oblique reflection coefficient of acoustic materials, *SAE* 2005.
[47] R. Lanoye, H.-E. De Bree, W. Lauriks, G. Vermeir, A practical device to determine the reflection coefficient of acoustic materials in situ based on a Microflown and microphone sensor, *ISMA*, 2004.
[48] E.H.G. Tijs, H.-E. De Bree, T.G.H. Basten, M. Nosko, Non-destructive and in-situ acoustic testing of inhomogeneous materials, Paper presented at the *33rd European Rotorcraft Forum*, Kazan, Russia, 11 September 2007.
[49] M.L. Shur, P.R. Spalart, M.K. Strelets, Noise prediction for increasingly complex jets, Part I: methods and tests, *International Journal of Aeroacoustics* 4 (2005) 213–246.
[50] C.L. Morfey, M.C.M. Wright, Extensions of Lighthill's acoustic analogy with application to computational aeroacoustics, *Proceedings of the Royal Society A* 463 (2007) 2101–2127.
[51] K.K. Ahuja, H. Tanna, B.J. Tester, Effect of simulated forward flight on jet noise, shock noise and internal noise, AIAA paper 79-0615, 1979.
[52] B.J.R. Thornber, D. Drikakis, R.J.R. Williams, D. Youngs, On entropy generation and dissipation of kinetic energy in high-resolution shock-capturing schemes, *Journal of Computational Physics* 227 (2008) 4853–4872.
[53] N. Forestier, L. Jacquin, P. Geffroy, *Journal of Fluid Mechanics* 475 (2003) 101–144.
[54] F. Farassat, K.S. Brentner, Supersonic quadrupole noise theory for high-speed helicopter noise, *Journal of Sound and Vibration* 218 (1998) 481–500.
[55] S. Ianniello, New perspectives in the use of the Ffowcs Williams–Hawkings equation for aeroacoustic analysis of rotating blades, *Journal of Fluid Mechanics* 570 (2007) 79–127.
[56] B.P. Murray, P. Ferrante, A. Scofano, Manufacturing Process and Boundary Layer Influences on Perforate Liner Impedance, AIAA Paper 2005-2849, 2005.
[57] D. Casalino, M. Genito, Turbofan aft noise predictions based on the Lilley's wave model, *AIAA Journal* 46 (1) (2008) 84–93.
[58] M. Genito, D. Casalino, Numerical modelling of sound diffraction at a half plane trailing edge, *AIAA Journal* 46 (4) (2008) 958–966.
[59] D. Blacodon, G. Elias, Level estimation of extended acoustic sources using a parametric method, *Journal of Aircraft* 41 (6) (2004) 1360–1369.
[60] J. Anthoine, J.-B. Gouriet, P. Rambaud, Reduction of the sonic boom from a high-speed train entering a gallery, AIAA-2007-3559, *13th AIAA/CEAS Aeroacoustics Conference*, Rome, Italy, 21–23 May 2007.
[61] C. Pierce, P. Moin, Progess-variable approach for large-eddy simulation of non-premixed turbulent combustion, *Journal of Fluid Mechanics* 504 (2004) 73–97.
[62] T.Ph. Bui, M. Ihme, M. Meinke, W. Schröder, H. Pitsch, Numerical Investigation of Combustion Noise and Sound Source Mechanisms in a Non-premixed Flame using LES and APE-RF. AIAA Paper 2007-3406, *13th AIAA/CEAS Aeroacoustics Conference*, Rome, Italy, May 2007.
[63] O. Macke, R. König, *Lärmminderungspotential und Fliegbarkeit von steilen Anflügen*, DLR Institut für Flugsystemtechnik, Braunschweig, Juli 2007.

[64] S. Guérin, U. Michel, Aero-engine noise investigated from flight tests, AIAA/CEAS Paper 2006-2463, May 2006.
[65] W. Dobrzynski, H. Buchholz, S. Guérin, G. Saueressig, U. Finke, Airframe noise characteristics from flyover measurements and predictions, AIAA/CEAS Paper 2006-3008, May 2006.
[66] ⟨http://www.fv-leiserverkehr.de/pdf-dokumenten/1600DLRAT-TA.pdf⟩.
[67] M. Diez, U. Iemma, V. Marchese, A Sound-Matching-Based Approach for Aircraft Noise Annoyance Alleviation via MDO, *13th AIAA/CEAS Aeroacoustic Conference*, Roma, AIAA Paper 2007-3667, May 2007.
[68] M. Diez, U. Iemma, Robust optimization of aircraft life-cycle costs including the cost of community noise, *13th AIAA/CEAS Aeroacoustic Conference*, Roma, AIAA Paper 2007-3668, May, 2007.
[69] U. Iemma, M. Diez, Multidisciplinary design optimization of aircraft under sound quality requirements, *International Journal of Aeroacoustics*, submitted for publication.
[70] S. Chan, X. Zhang, S. Gabriel, The attenuation of cavity tones using plasma actuators, *AIAA Journal* 45 (7) (2007) 1525–1538.
[71] X. Huang, S. Chan, X. Zhang, S. Gabriel, An atmospheric plasma actuator for aeroacoustic applications, *IEEE Transactions on Plasma Science* 35 (3) (2007) 693–695.
[72] X. Huang, S. Chan, X. Zhang, S. Gabriel, Variable structure model for flow-induced tonal noise control with plasma actuators, *AIAA Journal* 46 (1) (2008) 241–250.
[73] T. Salava, Program SPAD and its use in noise abatement of propeller airplanes, *Czech Aerospace Proceedings*, No. 3, 2006, pp. 14–18.
[74] B.J.R. Thornber, D. Drikakis, R.J.R. Williams, D. Youngs, An improved reconstruction method for compressible flows with low Mach number features, *Journal of Computational Physics* 227 (2008) 4873–4894.